METHODS TO MEASURE, PREDICT AND RELATE FRICTION, WEAR AND FUEL ECONOMY

Project Number	**R010902**
Document Number	**RD18-001067-1**
Date	**19 March 2018**
Award Number	**DE-EE0006793**

Principle Investigator	Steve P. Gravante, Ph. D.
Contributors	George Fenske, Nicholas Demas, Robert Erck Argonne National Lab 9700 S. Cass Ave. Lemont, IL 60439
Approved	Steve P. Gravante, Ph. D. Technical Specialist Engineering Services

EXECUTIVE SUMMARY

High-fidelity measurements of the coefficient of friction and the parasitic friction power of the power cylinder components have been made for the Isuzu 5.2L 4H on-highway engine.

In particular, measurements of the asperity friction coefficient were made with test coupons using Argonne National Lab's (ANL) reciprocating test rig for the ring-on-liner and skirt-on-liner component pairs. These measurements correlated well with independent measurements made by Electro-Mechanical Associates (EMA).

In addition, surface roughness measurements of the Isuzu components were made using white light interferometer (WLI). The asperity friction and surface characterization are key inputs to advanced CAE simulation tools such as RINGPAK and PISDYN which are used to predict the friction power and wear rates of power cylinder components.

Finally, motored friction tests were successfully performed to quantify the friction mean effective pressure (FMEP) of the power cylinder components for various oils (High viscosity 15W40, low viscosity 5W20 with friction modifier (FM) and specially blended oil containing consisting of PAO/ZDDP/MoDTC) at 25, 50, and 110 °C.

Ricardo's objective is to use this data along with advanced CAE methods to develop empirical characterizations of friction and wear mechanisms in internal combustion engines such that the impact of such mechanisms of engine fuel consumption and/or vehicle fuel economy can be estimated.

The value of such predictive schemes is that if one knows how a particular friction reduction technology changes oil viscosity and/or the friction coefficient then the fuel consumption or fuel economy impacts can be estimated without the excessive cost of motored or fired engine tests by utilizing cost effective lab scale tests and in combination with advanced analytical methods.

One accomplishment made during this work was the development and validation of a novel technique for quantifying wear using data from WLI through the use of bearing area curves (BAC). Long term wear testing was performed for a single combination of ring, liner and a low viscosity oil to illustrate the calculation of wear rate coefficients using this technique.

Unfortunately, advanced CAE modeling using RINGPAK/PISDYN and the fired engine friction measurements could not be completed.

As of mid-2017, Isuzu, the partner for supplying the engine and engine components for testing, had not provided the data and information needed to conduct the advanced CAE simulations (thermal FEA, structural FEA, RINGPAK and PISDYN) described in subtasks 2.1.3 and 3.1.3. This has lead both the DOE and Ricardo to believe that it is no longer possible to get this information and as a result Ricardo will not be able to achieve all of the technical milestones of the project.

After consultation with the DOE on 25 August 2017 and an internal review, Ricardo has confirmed that it is unlikely to complete all of the technical milestones and has decided to close the project effective 15 October 2017. Ricardo has committed to finish the low and high speed motored friction testing prior to this date in order to complete subtasks 2.1.1 and 2.1.2. As a consequence, subtasks 1.1.5, 2.1.3, 3.1.2, 3.1.3, and 3.1.4 have not been completed.

Ricardo officially informed DOE of this decision on 28 September 2017 and the DOE acknowledged this decision on 13 October 2017.

As consequence, Ricardo could not develop its predictive methodology for estimating the impact of friction reduction technologies on real world fuel economy.

PROJECT ACCOMPLISHMENTS

Milestone	Type	Description	Status
Friction and Wear Model Development – Test Conditions Defined	Technical	Stribeck Map to Guide Subsequent Lab-Scale Testing	Complete
Friction and Wear Model Development – Initial Data Set	Technical	Conduct Lab-Scale Testing and Develop New/Improved Friction and Wear Models	Complete
Friction Modifier	Go/No Go	Friction Modifier to be used in Task 2 and Task 3	Complete
Friction and Wear Model Development – Validation	Technical	Modeling and Simulation Best Practice for Lab-Scale Friction	Complete
Extension of Friction Model to a Motored Engine	Technical	Conduct Motored Engine Friction Testing	Complete
Modeling and Simulation for Motored Engine Friction	Technical	Modeling and Simulation Best Practice for Motored Engine Friction	Incomplete
Hardware Combinations	Go/No Go	Hardware combinations for long term wear testing	Complete
Extension of Friction Model to a Fired Engine	Technical	Conduct Fired Engine Friction Testing	Incomplete
Modeling and Simulation for Fired Engine Friction	Technical	Modeling and Simulation Best Practice for Fired Engine Friction	Incomplete
Wear Model Development	Technical	Conduct Lab-Scale Wear Testing	Complete
Wear Model Development	Technical	Correlation of Lab-Scale Wear to Dyno or Vehicle Wear	Incomplete
Wear Model Development	Technical	Modeling and Simulation Best Practice for Dyno or Vehicle Wear	Incomplete
Reporting	Technical	Submit Final Report	Complete

TABLE OF CONTENTS

1 INTRODUCTION 6
2 OBJECTIVES 6
3 APPROACH 7
4 RESULTS 9
4.1 Subtask 1.1.1 – Create Model of Lab-Scale Setup 9
4.2 Subtask 1.1.2 – Develop Engine Stribeck Map 11
4.3 Subtask 1.1.3 – Lab-Scale Component Testing at ANL 14
4.4 Subtask 1.1.4 – Full-Scale Component Testing at EMA 31
4.5 Subtask 1.1.5 – Develop Lab-Scale Data Correlation 34
4.6 Subtask 1.1.6 – Development and Validation of RINGPAK Modelling Best Practice of a Lab Scale Test 35
4.7 Subtask 2.1.1 & 2.1.2 – Low and High Speed Motored Engine Friction Measurements 38
4.8 Subtask 2.1.3 – Motored Engine RINGPAK and PISDYN Modelling 47
4.9 Subtask 3.1.1 – Thermal Survey of Fired Engine 49
4.10 Subtask 3.1.2 – Fired Engine Friction Tests 53
4.11 Subtask 3.1.3 – Fired Engine RINGPAK and PISDYN Modelling 53
4.12 Subtask 3.1.4 – Development of Empirical Models for Prediction of Real World Fuel Economy 56
5 PRODUCTS DEVELOPED 57
6 CONCLUSIONS 57
7 RECOMMENDATIONS 58
8 REFERENCES 59
APPENDIX 1 DESCRIPTION OF ZYNP COMPONENTS TESTED 60
APPENDIX 2 DESCRIPTION OF EMA-LS9 RING AND CYLINDER WEAR TESTER 62
APPENDIX 3 PROJECT PARTNERS AND ROLES 63
APPENDIX 4 VISCOSITY OF OILS TESTED 64

METHODS TO MEASURE, PREDICT AND RELATE FRICTION, WEAR AND FUEL ECONOMY

1 INTRODUCTION

A Funding Opportunity Announcement (FOA) was issued on January 24th, 2014 (DE-FOE-0000991). This FOA is supported by the Vehicle Technologies Office (VTO) in the Department of Energy (DOE) with the following objectives:

- Reduce the usage of highway petroleum by 1.4 million barrels per day by 2020.
- Develop cost-effective technologies to improve vehicle fuel efficiency and achieve or exceed corporate average fuel economy (CAFE) standards of 144 gCO2/mile (61.6 miles per gallon) for cars and 203 gCO2/mile (43.7 miles per gallon) for light trucks by 2025.

Fourteen (14) Areas of Interest (AOI) that focus on advanced light-weighting, advanced battery development, power electronics, advanced heating, ventilation, air conditions systems and fuels and lubricants make up the scope of the FOA. Ricardo along with Argonne National Lab requested funding under AOI 11B.

AOI 11 is concerned with powertrain friction and wear reduction. According to the FOA, parasitic losses within vehicle powertrains (engine and transmission) account for approximately two million barrels of oil consumption per day in the US.

Under topic 11 there are two subtopics: 11A and 11B. Subtopic 11A is concerned with the development and demonstration of friction and wear reduction technologies for light-, medium- and heavy-duty vehicles.

Subtopic 11B, for which this grant has been issued, is concerned with the identification and quantification of friction losses along with methods to measure and predict fuel economy gains in full engines and/or vehicles.

- Ricardo's objective is to use this data along with advanced CAE methods to develop empirical characterizations of friction and wear mechanisms in internal combustion engines such that the impact of such mechanisms of engine fuel consumption and/or vehicle fuel economy can be estimated.
- The value of such predictive schemes is that if one knows how a particular friction reduction technology changes oil viscosity and/or the friction coefficient then the fuel consumption or fuel economy impacts can be estimated without the excessive cost of motored or fired engine tests by utilizing cost effective lab scale tests and in combination with advanced analytical methods.

2 OBJECTIVES

To develop characterizations of friction and wear mechanisms in internal combustion engines and methods to predict the impact of such mechanisms on engine fuel

consumption or vehicle fuel economy respectively. The methods of prediction will be both empirically and analytically based.

- Fundamental tribological parameters will be measured using lab-scale tests.
- Changes in engine friction will be calculated using CAE methods based on input provided from the lab-scale tests and validated against motored friction tests.
- Changes to brake specific fuel consumption will be measured in a real engine.
- Empirical correlations will be established that allows for estimating changes in brake specific fuel consumption (BSFC) based on engine power and speed and changes in friction power computed from the CAE methods.
- Empirical models will be integrated to derive vehicle fuel economy benefits.
- In a similar way, component wear will be analyzed and predicted.

3 APPROACH

Ricardo's technical approach begins with acquiring a detailed and high-fidelity dataset of the friction and wear characteristics of typical power cylinder components, e.g., piston ring, liner and piston skirt.

The piston ring, liner and piston combination will be from the Isuzu 4H engine whose specifications are summarized in Figure 1.

Isuzu 4H Engine

- U.S. EPA On Highway 2010 Standards
- Displacement: 5.2 L (317 in.^{3})
- B = 115 mm, Stroke = 125 mm
- Turbocharged intercooled diesel
- Peak torque: 441ft-lbs. @ 1,850 rpm
- Engine Power: 210 HP @ 2,500 rpm
- Fuel consumption: 143 mm3/stroke
- CO2: 561 / 534 g/bhp-hr FTP/RMC
- Oil Capacity: Oil only 7.5 liters/7.9 quarts and Oil and filter 8.2 liters/8.7 quarts
- Oil Type: CJ-4 Shell Rotella T5 40W, e.g., 15W40
- Electric & self-priming fuel lift pump
- 12V
- Glow plug starting aid
- High angularity oil pan
- 10,000 mile or every 12 month (CJ-4:W-40)
- Warranty 3-year / Unlimited Miles

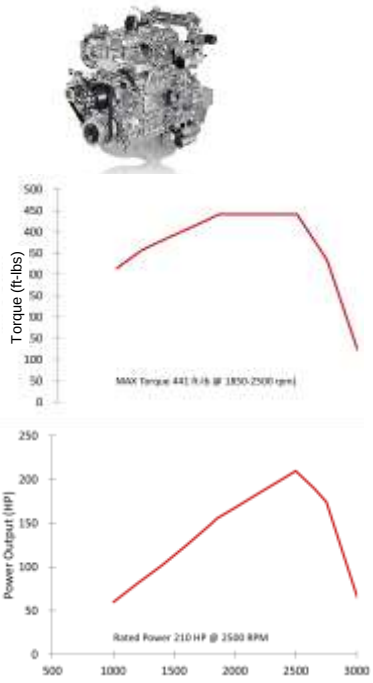

Figure 1 Isuzu 4H Engine Specifications.

The friction and wear characteristics will be measured for ring-on-liner and piston-skirt-on-liner configurations in combination with typical friction and/or wear reduction technologies such as a low viscosity oil, friction modifying oil additives and coatings.

The dataset will be obtained by using the same components and friction/wear reduction technologies through a progression of control tests each with its own pros and cons for quantifying friction and wear. These include lab-scale bench tests using a reciprocating test rig (Adjustable Angle Reciprocating Tester or AART) at Argonne National Lab (See Figure 2), motored dyno tests and fired engine tests at Ricardo.

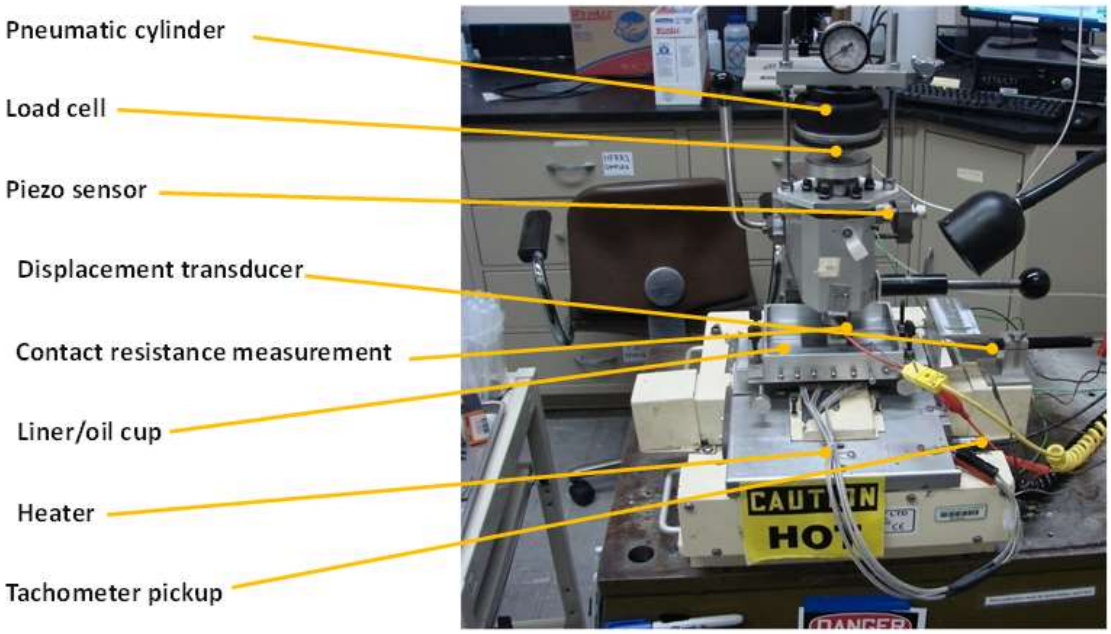

Figure 2 Picture of the AART at Argonne National Lab.

The data obtained will be used as follows:

- To provide necessary inputs to CAE simulations of the engine power cylinder for friction and wear prediction.
- To provide data for validation of CAE methods used for the prediction friction and wear.
- To establish wear rate coefficients for the prediction of wear.

As previously stated, calculated changes in friction and wear will be used to develop scaling factors for estimating drive cycle specific fuel consumption and component wear.

4 RESULTS

4.1 Subtask 1.1.1 – Create Model of Lab-Scale Setup

4.1.1 Task Details

A model of the lab-scale test rig at Argonne National Lab (AART) will be developed using Ricardo's RINGPAK software. This task also entails the initial verification that the model is working as expected. The model will be used in a later task to simulate the various lab-scale tests performed in order to validate the model inputs and establish the best practice for modeling the lab-scale test in RINGPAK.

4.1.2 Task Summary

A RINGPAK model was developed to simulate the reciprocating motion of ANL's lab-AART rig. Figure 3 shows a schematic of the lab-scale ROL test configuration:

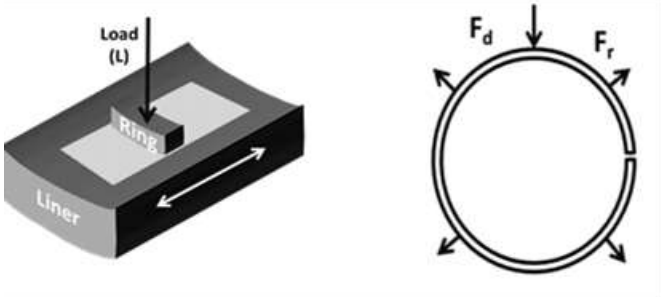

Figure 3 Ring-on-Liner test configuration; radial and diametrical tension definition in RINGPAK.

The ROL RINGPAK model simulates the applied normal load (L) by controlling the ring tension, F_d. To replicate the sinusoidal motion of the ROL test rig within RINGPAK, a long crank coupled with a short crank throw is imposed on the RINGPAK model to provide a stroke comparable to ROL test rig (i.e., 20 mm). Typical operating conditions and the corresponding simulation boundary conditions for the ROL test rig and ROL RINGPAK simulation are given in Table 1.

Table 1 Lab-Scale and RINGPAK test conditions and equivalent loads/ring tensions.

	ROL Test				ROL RINGPAK			
Rotational Speed	0 – 300 rpm				0 to 3600 rpm			
Load (N)	15	50	100	250	-	-	-	-
Load (N/mm) for a 15 mm contact path	1	3.3	6.7	16.7	-	-	-	-
Equivalent Radial Force, Fr (N)	358	1194	2388	5969	358	1194	2388	5969
Equivalent Ring Tension, Fd (N)	-	-	-	-	117	390	779	1948

The ROL RINGPAK model simulates the ROL test conditions through the appropriate selection of the ring tension, F_d. Experimentally, the ROL rig uses (normal) loads ranging from 15 N to 250 N (with loads up to 2000 N possible) and a contact region of 10 to 15 mm wide (typical). This results in a load per unit width of 1 to 17 N/mm. For a 115 mm bore, this load range would be equivalent to total radial force from 358 to 5969 N. The equivalent diametric ring tensions that should be used in the RINGPAK simulations were calculated using the following relationship:

$$F_r = 2\pi F_d / 2.05$$

Although the equivalent ring tensions in Table 1 are high compared to typical HDD rings (F_d = 25 to 50 N), gas pressure during the combustion cycle can increase the radial force dramatically to produce unit loadings near 50 N/mm (i.e., F_r in excess of 15kN).

The ROL RINGPAK model includes all of the essential engine geometries and typical material properties of the Isuzu engine that will be used in subsequent motored and fired dyno tests. Simulation results show similar behavior as the ROL tests (see Figure 4) indicating the validity of the approach to model the short stroke reciprocating motion of the AART rig in RINGPAK. The square wave prediction of RINGPAK is the result of improper specification of simulation boundary conditions. This issue is further explained and correlation is improved under the subtask 1.1.6.

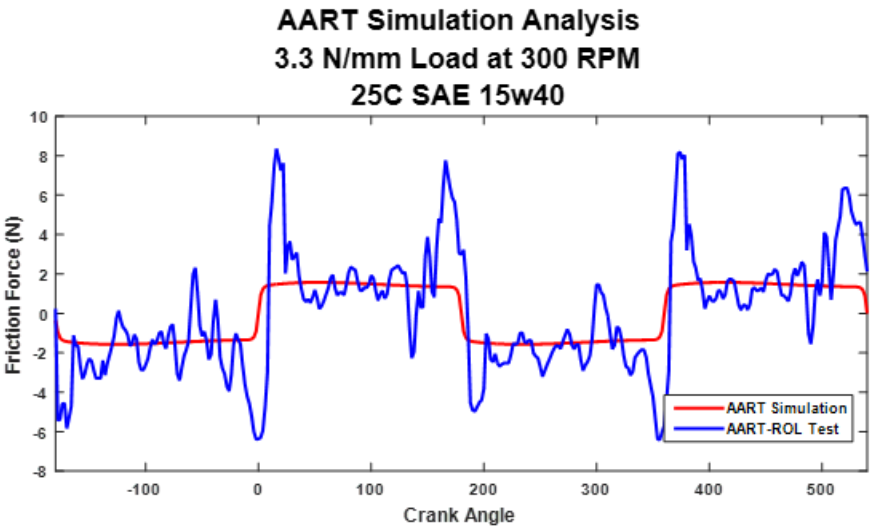

Figure 4 Results from ROL RINGPAK simulation using Isuzu geometries, typical material properties, and generic 15W40 oil properties.

4.2 Subtask 1.1.2 – Develop Engine Stribeck Map

4.2.1 Task Details

This task entails the mapping of Stribeck parameter as a function of engine speed and load for a typical diesel engine. It will be used to identify the friction regime in which the engine is operating as a function of speed and load to guide the development of an appropriate test matrix for the lab-scale bench tests and engine dyno tests.

4.2.2 Task Summary

To simulate the AART rig it is valid to assume a constant temperature as a function of position/crank-angle. However, the temperature from the top to the bottom of the liner is not constant which is indicated in Figure 5.

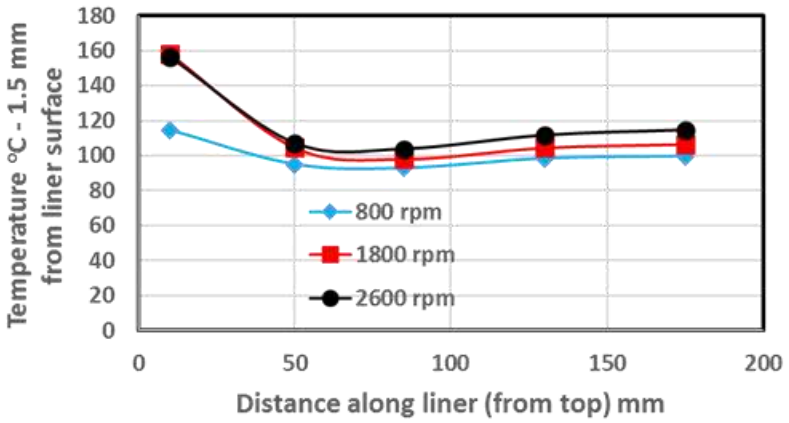

Figure 5 Axial variation of cylinder temperature at three speeds.

Figure 5 shows the measured liner temperature (measured 1.5 mm from the inner surface of the cylinder) as a function of distance from the top of the cylinder. The data at each location are averages obtained from four separate cylinders at different circumferential locations (a total of 7 measurements). The temperature data at 1800 rpm (30 Hz) was used to calculate the Stribeck number as a function of crank angle where the Stribeck number is defined as:

$$Str.\# = \eta S/L$$

Where: η = viscosity (Pa-s)
S = speed (m/s)
L = Load (N/m)

Figure 6 shows the results of the calculations of the Stribeck number as a function of crank-angle for a motored (low load) and fired (full load) engine running @ 1800 rpm (30 Hz). The solid black curve shows calculations under low load conditions, while the solid red curve shows calculated Stribeck numbers under full load. The dashed blue line shows calculations at full load assuming a constant liner temperature of 99.8 °C (the average liner temperature at 1800 rpm). Note the peak Stribeck number for the data in Figure 6 is approximately 3×10^{-4} under low load conditions.

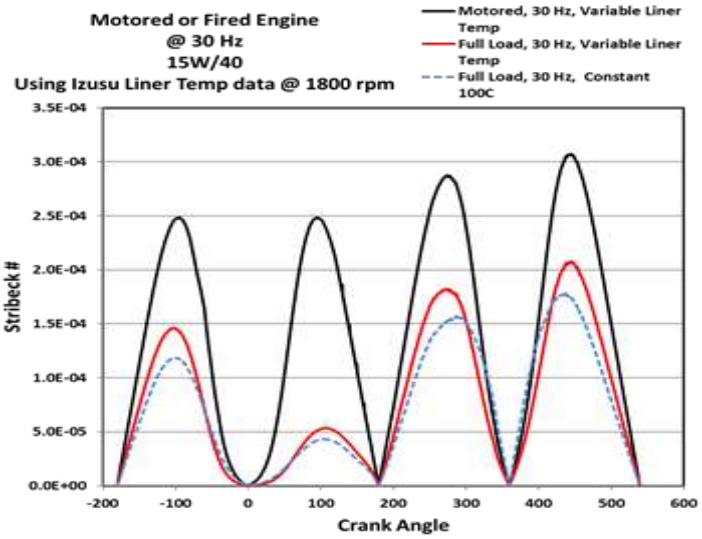

Figure 6 Stribeck number as a function of crank angle for 15W/40 oil under motored and fired conditions assuming axial temperature profile in Figure 5.

For comparison, Figure 7 shows Stribeck numbers for benchtop simulations at 20 and 100 °C at 5 N/mm and 25 N/mm ring loading. Temperature has a big impact on viscosity (236 mPa-s @ 20 °C vs. 11.2 mPa-s at 100 °C – a factor of 20), while load changes from 25 to 5 N/mm – a factor of 5. Together the peak Stribeck numbers differ by a factor of 100 just between the different benchtop conditions. Note the peak Stribeck number for the benchtop simulations is approximately 1.5 x 10^{-5}.

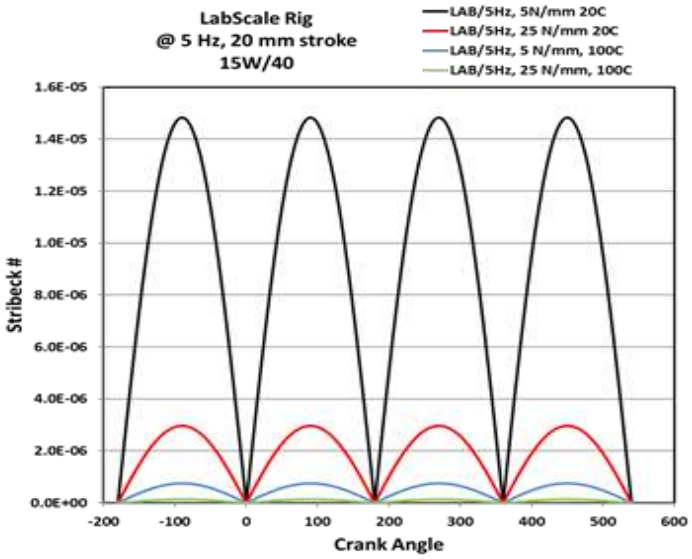

Figure 7 Stribeck number as a function of crank angle for 15W/40 oil for benchtop conditions.

Figure 8 summarizes the ranges of Stribeck numbers one can expect to encounter with benchtop and engine rigs for different conditions. The Stribeck numbers range from the

low 10^{-9} s for a benchtop test at 100 °C at high load to the mid 10^{-3} s for high speed motored engine run at room temperature.

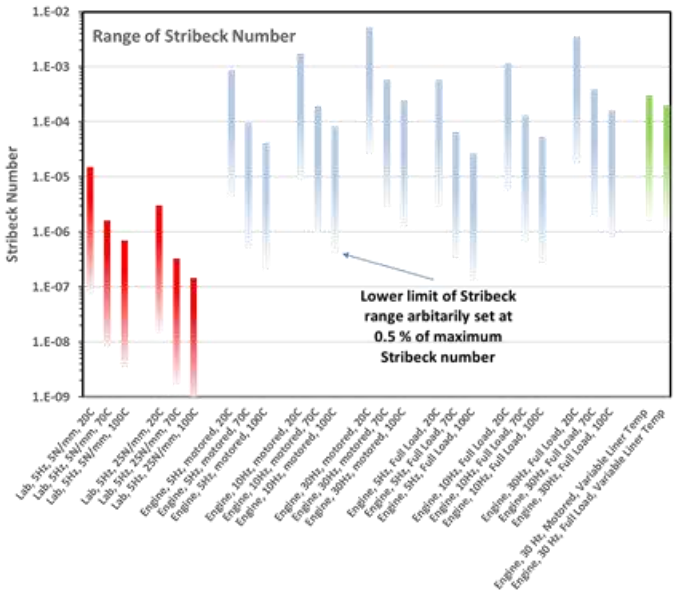

Figure 8 Range of Stribeck numbers expected for benchtop and engine tests that simulate ring-on-cylinder bore conditions.

The results suggest a poor overall replication of the Stribeck conditions between the benchtop tests and an actual fired, or, motored engine rig due in large part to the differences in the maximum speeds typically available in benchtop simulations.

However, the best overlap appears to be at the low load, room temperature benchtop operation (5 Hz, 5 N/mm, 20 °C) and the motored condition at 5Hz (300 rpm), 100 °C, or, full Load at 30 Hz (1800 rpm), 100 °C.

Therefore, motored friction tests will target measurements as close to 300 rpm as possible.

4.3 Subtask 1.1.3 – Lab-Scale Component Testing at ANL

4.3.1 Task Details

A test matrix which identifies the number of hardware combinations and the range of contact loads, relative velocities and oil viscosities to be tested will be developed. The test matrix will be executed using samples cut from actual components, e.g., rings, liners, pistons. This testing will provide the needed data for subsequent tasks as well as facilitate comparison to full component lab-scale test results at EMA (subtask 1.1.4).

4.3.2 Task Summary

One of the primary deliverables of this task is to identity the appropriate friction modifier (FM) to be used in subsequent testing, e.g., full component lab-scale tests, engine tests, etc.

Table 2 shows all of the oil combinations tested. A number of iterations were necessary to determine the two final candidate oils which will be used in subsequent testing.

Table 2 Description of Oil + FM Evaluated.

Oil	Description	Tests performed	Naming
Batch 1 oils	2 high vis HDDO oils (15W/40) - one with no Fm, one with a high FM treat	Ring-on-Liner and Ball-on-Flat	IM15023-2
	2 low-vis HDDO oils (5W/20) - one with, one without FM	Ring-on-Liner and Ball-on-Flat	
Batch 2 oils	4 PCMO 5W/20 oils (1-4) with different FMs	Ball-on-Flat	E01031-074
	4 HDDO 5W/20 oils (5-8) with different FMs	Ball-on-Flat	
Batch 3 oils	2 PCMO variants of PCMO oil 3 (3a and 3b) with different FM chemistry and treat rate	Ball-on-Flat	E00365-698
Batch 4 oils	6 PCMO 5W/20 oils (1, 2, 3, 3a, 3b, 4) - confirmtaion blends	Ball-on-Flat	E00365-708
	4 HDDO 5W/20 oils (5-8) - confirmation blends	Ball-on-Flat	

Batch 1 consisted of blends of a low- and high-viscosity oil with and without a FM. Batch 1 testing showed that the FM treat rate used had minimal impact on friction. It was then decided to re-blend the oils using a PCMO additive package to achieve additional friction reduction which became Batch 2. Batch 2 testing showed a measurable difference between 15W/40 HDDO and 5W/20 PCMO for oil 3. An attempt was made to gain further friction reduction by optimizing the treat rate for oil 3, i.e., oils 3a and 3b in Batch 3. However, oils 3a and 3b showed very little improvement in friction reduction. At this point it was realized that a blending error had occurred in Batches 2 and 3 that necessitated the re-blend of all of the oils: 1, 2, 3, 3a, 3b, 4, 5, 6, 7, 8.

The re-blending led to Batch 4. Batch 4 testing showed significant differentiation in the friction response between HDDO high-vis (15W/40) No FM oil (baseline) and HDDO (5W/20) High FM oil 7. This testing led to the selection of the final two engine oil candidates for subsequent testing which are summarized in the table below (Table 3).

Table 3 Specification of engine oils to be used in subsequent testing.

Blend	15W40 no FM	5W20 High FM
Code main name	IM1502322-A-001	E00365-708-7
Description	No FM	High FM
Estimated Viscosity Grade	15W-40	5W-20
Formulation	HDD	HDD
kv100 (cSt)	14.30	7.46
CCS temperature deg C	-20	-30
CCS (cP)	3890	5018

Figure 9 illustrates the impact of the friction modifier on the boundary coefficient friction. From the figure, it can be seen that 25% reduction in the friction coefficient and a 48% reduction in oil viscosity has been achieved.

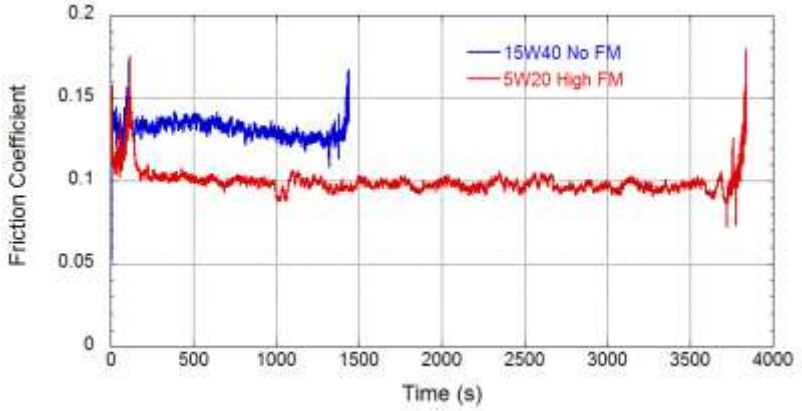

Figure 9 Effect of friction modifier on the boundary friction coefficient.

Figure 10 shows a summary table of the boundary friction measurements for both ring-on-liner and skirt-on-liner configurations. The values of μ_{asp} summarized in the figure will be used as a direct input into the RINGPAK model. In addition to μ_{asp}, crank angle resolved coefficient of friction measurements were also obtained. The crank angle resolved data will be used to facilitate the calibration and validation of the RINGPAK model. See subtask 1.1.6 for an example of the crank angle resolved coefficient of friction and the status of the modeling efforts.

Ring/liner

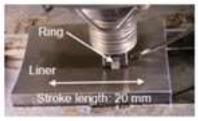

Temperature (°C)	70		100		130	
Load (N)	50	250	50	250	50	250
15W40 no FM	0.130	0.126	0.133	0.136	0.138	0.132
5W20 high FM	0.088	0.092	0.102	0.097	0.097	0.098

Skirt/liner

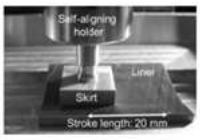

Temperature (°C)	70		100		130	
Load (N)	50	250	50	250	50	250
15W40 no FM	0.177	0.174	0.168	0.177	0.177	0.170
5W20 high FM	0.092	0.093	0.086	0.086	0.084	0.089

Figure 10 Summary of boundary friction coefficients for ring-on-liner and skirt-on-liner tests with the baseline Isuzu components.

An interesting observation was made while conducting the skirt-on-liner tests. Specifically, the skirt-on-liner tests failed to show a steady-state value for the boundary coefficient at the end of the standard duration test. This behavior was also observed during the full-scale testing (see Task summary under subtask 1.1.4).

This led to longer duration (24-hour vs. 1-hour) tests being conducted. The 24-hour test was run twice. The first time the test was allowed to run continuously for 24 hours while recirculating the same oil. The second time the test was stopped periodically so that the oil could be refreshed. Results for these tests are shown in Figure 11 below.

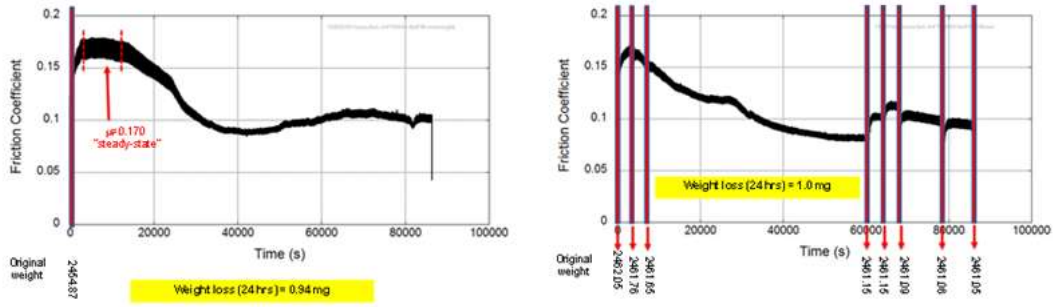

Figure 11 Outcome from long duration skirt-on-liner tests.

From the results, it can be seen that

1. An initial steady-state was reached but then μ_{asp} fluctuated
2. Boundary friction appears to vary according the tribochemical film formation (a very dynamic process based on additive chemistry interactions), and material changes (graphite/resin exposure on the skirt)
3. These changes are driven at rates proportional to temperature and load
4. Though outside the scope of this task, this phenomenon probably should be considered when validating models against physical tests because if μ_{asp} is dependent on the integral of effects over time then model inputs must then correspond to the history of the engine or test coupon one is attempting to model.

Reciprocating tribometer tests with the coated Isuzu pistons and rings

Uncoated Isuzu liner test coupons were sent out to C2D to be coated with a DLC coating. When the coated liner coupons were received, segments were extracted and tests were performed to evaluate the friction behavior of the coated liner against uncoated rings. There was only a limited number of tests performed using the coated liners because there was an adhesion issue with the coating. Two tests under 50 N and 70 ˚C using two coated samples with the C2D coating were performed for repeatability, and as shown on the image of Figure 12 for one of the segments, evidence of coating delamination can be seen. The other sample looked similar. The sliding direction in these images is left-to-right. The bright area corresponds to the substrate (cast iron liner).

Figure 12 A cast-iron liner segment coated with a DLC coating from C2D showing delamination.

Further examination using optical microscopy and profilometry confirmed delamination is shown in Figure 13. The dark areas correspond to the coating.

Figure 13 Micrograph showing coating delamination.

The thickness of the coating which was approximately 10 microns was measured at the same area using optical profilometry (see Figure 14).

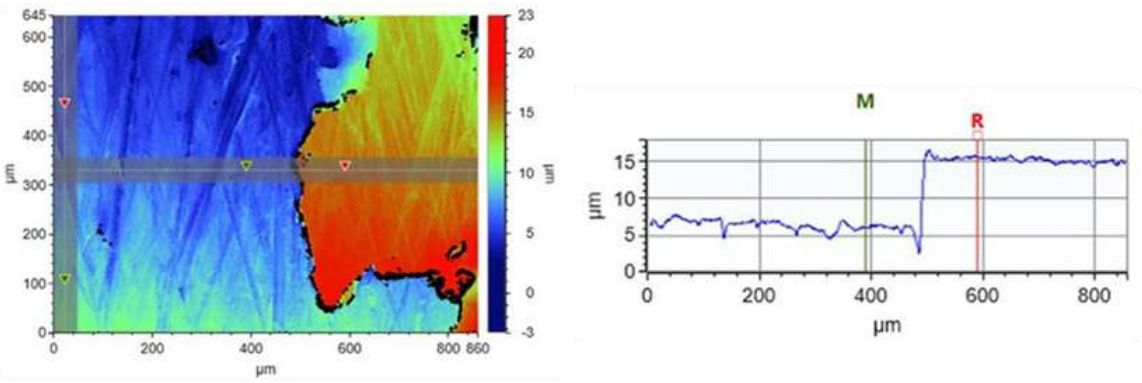

Figure 14 Profilometric measurement and corresponding line scan across delaminated area.

Rings were also sent to C2D for coating. The rings were examined upon receipt before testing using optical microscopy which showed that the coating did not adhere uniformly. The photo in Figure 15 shows that the rubbing edge of the top compression ring (which is the one subjected to wear in the reciprocating tests) is coated irregularly. The 2ng ring could not be coated due to adhesion issues, while the oil control ring (OCR) was coated irregularly.

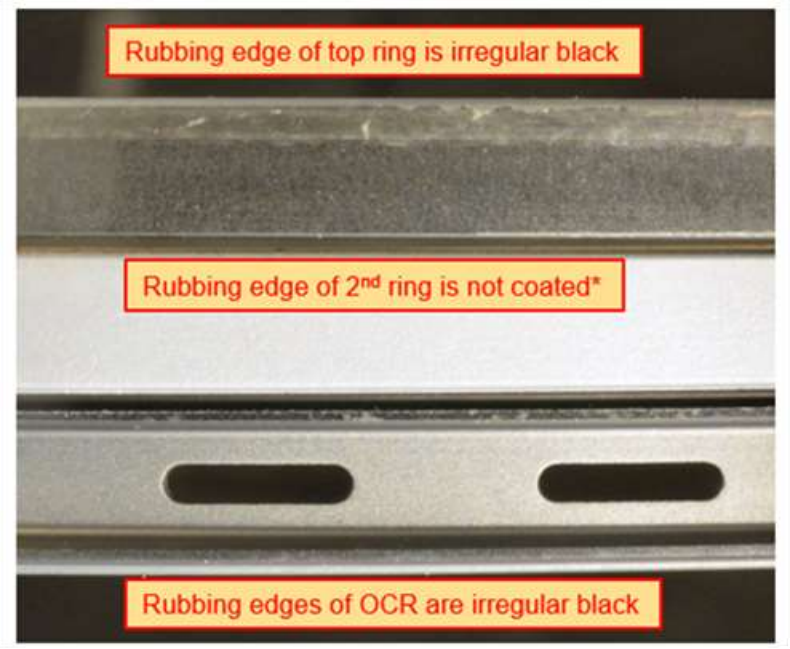

Figure 15 Photo of the three rings (top ring, 2nd ring, and OCR) after C2D attempted coating with a DLC coating.

Uncoated pistons were received by Isuzu in two sizes. These were nominal-sized and under-sized; 22 pistons were sent out to Orion to be coated with an MoS_2 coating. Ten

pistons were sent to Ricardo for engine testing and 6 were sent to EMA for evaluation. The rest were kept by ANL for tribological testing. One of the coated pistons was sectioned and segments were extracted for testing. Results show a high wear rate for this coating while the friction is comparable to the baseline Isuzu pistons, which are coated with Grafal, even though the MoS_2 coating was supposed to be a lower friction coating (see Figure 16) according to the supplier.

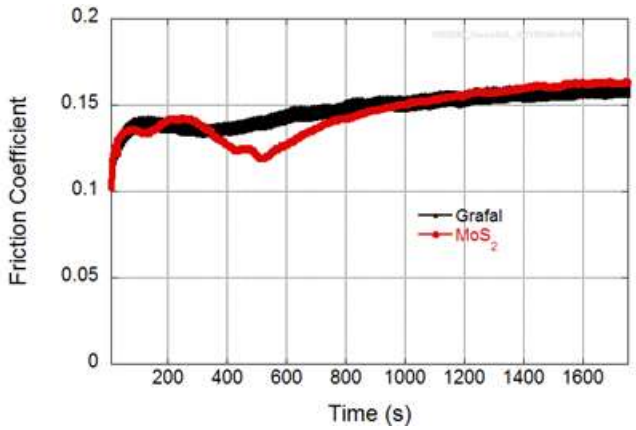

Figure 16 Comparison of friction coefficient as a function of time for two coated piston skirt segments.

The poor performance of these coatings has implications for the proposed test matrix. The original test matrix assumed the hardware builds shown in Table 4. Base refers to the original Isuzu piston/ring. New refers to the coated pistons and rings described earlier.

Table 4 Original engine build test matrix. Oil A = high viscosity, Oil B = low viscosity w/ FM.

Build	Ring	Piston	Oil
1	Base	Base	A
2	New	Base	A
3	Base	New	A
4	New	New	A
5	Build 1		B
6	Build 2, 3, or 4		B

Considering that coating development is an out-of-scope activity for the current project and that the project timing and budget cannot accommodate continued development of

coatings, Ricardo and ANL have decided to forego testing of any coated components. The implication of this setback is that builds 2, 3, 4 and 6 shown in Table 4 cannot be tested.

As a substitute, the project team added a special oil blend (not fit for commercial use because of missing additives which extend oil life) but which considerably reduces the boundary friction coefficient to the test matrix. Specifically, past research conducted by Argonne indicated that a semi-formulated oil (using a PAO coupled with ZDDP and MoDTC) consistently exhibits boundary friction coefficients in the range of 0.03/0.05. Though not commercially viable this special oil blend provides another means to change the engine friction and an excellent test case for validating our prediction methods.

Consequently, the engine builds that will be tested will be the following:

Table 5 New build test matrix. Oil A = high viscosity, Oil B = low viscosity w/ FM, Oil C = special blend.

Build	Ring	Piston	Oil
1	Base	Base	A
5	Build 1		B
7	Build 1		C

On 28 October 2016, Infineum agreed to provide oil samples to ANL so that the performance of the special oil blend could be verified on their reciprocating tribometer. On 29 November 2016, Infineum shipped oil samples to ANL which were received on 5 December 2016. Testing of the oil samples began immediately and finished on 22 December 2016. The results are summarized in the following table and were shared with Infineum at that time.

Table 6 Summary of lab-scale tests using Infineum's special oil blend.

Blend	COF
Infineum/Ricardo 15W/40 NO FM	0.13
Infineum/Ricardo 5W/20 High FM	0.10
ANL In-house PAO4 – ZDDP/MolyVan855	0.05 to 0.07
Honda Best	0.03
Infineum E01208-028-002 (ZDDP1 + Moly Trimer)	0.06
Infineum E01208-028-003 (ZDDP1 + high rate Moly Trimer)	0.06

The results indicate that the performance of either variant of oil blends was satisfactory and consistent with previous experience. It was then agreed that Infineum would blend

up 100 gallons of the E01208-028-002 sample and ship to Ricardo for use in the motored and fired engine friction tests.

Based on the positive observations from the lab-scale testing, the project team will proceed with the engine builds summarized in Table 5.

Accelerated Wear Testing

One of the key inputs to RINGPAK or PSDYN is surface roughness characteristics. These characteristics are described using the Greenwood-Trip (GWT) parameters which are derived from high fidelity surface profile measurements. It is through the GWT parameters that the contribution of surface asperities to friction force is accounted.

Considerable effort has been expended to determine the best way to acquire surface profiles using white light interferometry (WLI) and the best way to post-process surface images to obtain GWT parameters.

The following parameters were studied:

- Image magnification
- Low pass filter cut-off
- High pass filter cut-off/curvature removal

Based on sensitivity study, it was determined that the recommended parameters for image acquisition and post-processing are 10X magnification and 2.5 µm low pass filter. The sensitivity study showed that all methods for removing surface curvature produced equally good images.

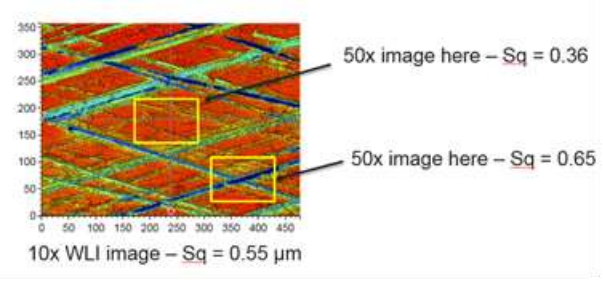

Figure 17 Difference in GWT parameters with different magnifications.

The 10X WLI magnification balances the need to retain detail yet obtain representative surface roughness for inhomogeneous surfaces such as honed cylinder liners. An image magnified 50X would provide an insufficient area to calculate representative surface roughness. See Figure 17 which shows the difference in surface parameters calculated with images of different magnification.

The setting for the low pass filter was based on the expected size of the asperity summits so that random noise within an individual pixel is not identified as a summit. This can be better understood when one considers that a perfectly smooth surface will have an

erroneously high summit count due to pixilation and the method by which the summit is defined. Thus, a filtering scale must be chosen to remove pixel-scale noise while revealing the true summit. Through estimations and trial and error it has been determined that a “real” summit is about 6 pixels in width or 2.5 µm.

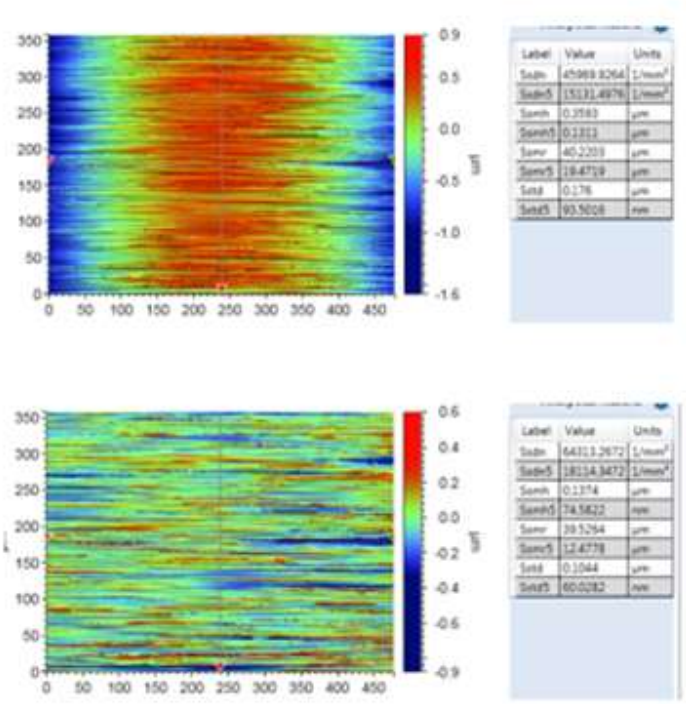

Figure 18 Difference in GWT parameters with and without surface curvature removed.

Finally, even though the method by which surface curvature is removed is not crucial. Surface curvature must be removed none-the-less. This conclusion was arrived at based on the difference in calculated surface parameters with and without surface curvature removed. Without surface curvature removed the surface mean height is estimated as larger than actual and thus the algorithm “misses” some asperity summit which artificially lowers the summit density resulting in inaccurate GWT parameters. See Figure 18.

The literature does not provide any information on how to measure liner wear. For this work, a new method to measure liner wear is proposed. In order to demonstrate its robustness, a real liner surface where the exact amount of wear could be determined was used. The original liner profile was mathematically processed such that features above a certain height were “cut”. This is demonstrated in Figure 19.

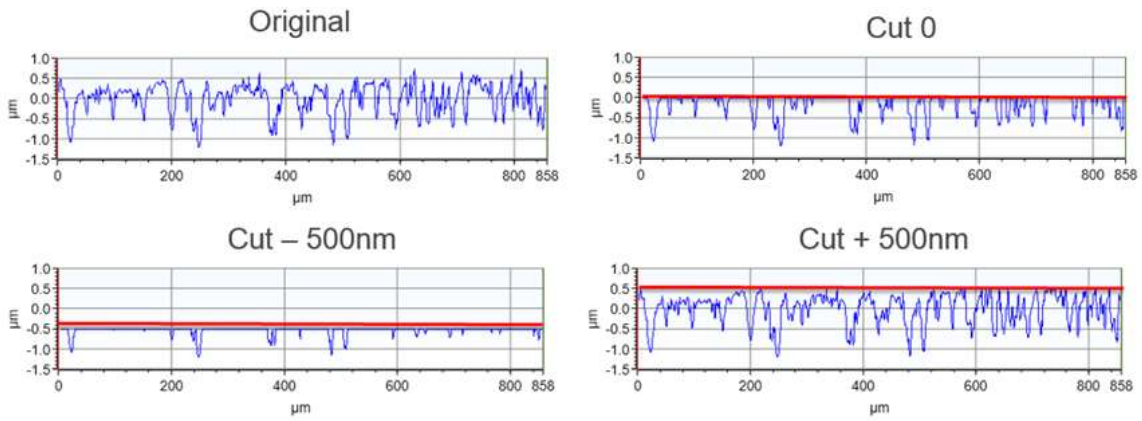

Figure 19 Profilometric line scans for a liner surface as-is and "cut" at certain heights.

If the profiles are subtracted from one another, a volume can be calculated which exactly corresponds to the volume of the material that has been removed. For a surface that has been worn, the profile before and after testing can be used to determine wear provided that the amount of wear remains low enough that the deepest honing grooves are largely unaffected. If a surface profile before testing is not available or cannot be measured, as in the case of a cylinder liner that was used in an actual engine, the same method can be applied successfully in a statistical manner outside the area of contact. Several profilometric measurements must be performed, and the deepest grooves (>85%) will have to be matched on the basis of the bearing area curve.

For the surfaces above, the corresponding bearing area curves (BAC) are shown in Figure 20 and indicate that the BAC might be a good way to differentiate between unworn and worn surfaces and, in particular, can be used to compute the volume of material removed provided that

- the same region is profiled before and after it is worn
- BACs are referenced to the same zero

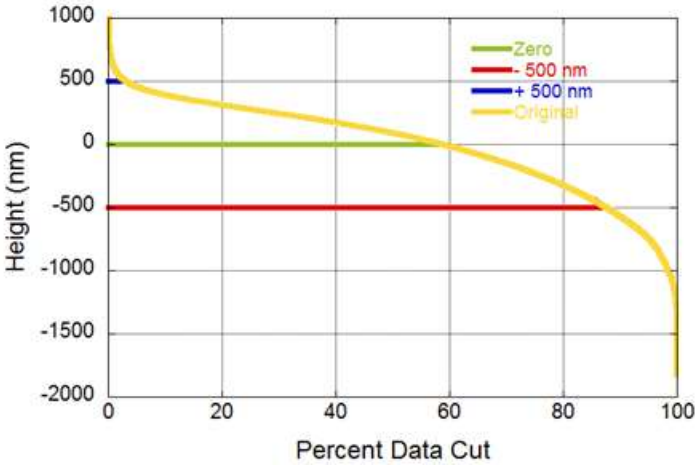

Figure 20 Bearing area curves for an original liner profile mathematically processed such as features above a certain height are "cut" at zero, -500 nm and 500 nm.

When the first condition can't be met, BACs can still be used to calculate the wear volume but in a statistical sense. That is, several regions of the unworn and worn surface can be profiled and their BACs averaged. The difference in the average unworn BAC and the average worn BAC then yields the average wear volume provided the second condition can be met.

A difficulty arises when trying to reference the BACs to the same zero since the white light interferometer doesn't measure the zero in an absolute sense. Instead, surface heights are referenced to the mean line which varies from one sample to another.

However, Stewart[1] indicated that two BACs can be vertically registered (i.e., referenced to the same zero) by adjusting the vertical height of the BAC such that the lower 20% of the BACs are matched. The validity of this approach assumes that the deepest parts of the surface should remain unaltered as wear mechanisms tend to remove the peaks in the surface leaving the valleys unaltered.

This hypothesis was tested by imaging a single liner segment which was progressively polished with sandpapers of varying grades to produce wear and the exact same area was imaged after each polishing event using the Bruker GTK white light interferometer.

Figure 21 below shows the images of the progressively worn surface:

[1] Stewart, M., **A New Approach to the Bearing Area Curve**, FC90-229, Society of Manufacturing Engineers, 1990.

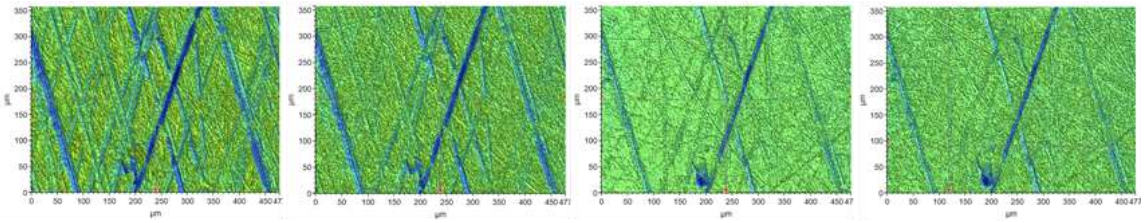

Figure 21 WLI images of a single liner segment after progressive polishing.

The BACs after a vertical adjustment is made such that the lower 20% is match is shown in Figure 22.

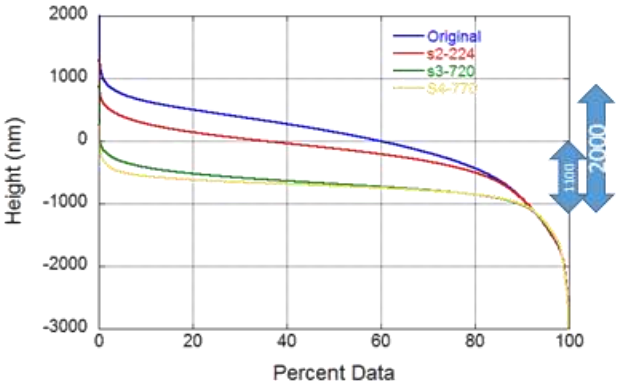

Figure 22 BACs of a progressively polished surface after the lower 20% is matched.

The area between the curves is proportional to the volume of material removed. Calculations show that 76,997 μm^3 of material has been removed by the polishing process described above.

How do we know that this value is correct? A simple calculation can show this to be the case. The BACs in Figure 22 show that the peaks were worn from about 2000 nm to about 1100 nm (where the lines converge). The area of the scanned image is 477 µm x 355 µm = 169,000 μm^2 so the volume of material removed from a block 900 nm tall (2000 – 1100 nm) would be ~152,000 μm^3. However, the topography is not a rectangular block but is more like a series of hemispheres representing the peaks and values of a surface. A hemisphere has a volume that fills 52% of the block that it is inside. Therefore, the lost volume of a hemisphere that is compressed from 2000 nm tall to 1100 nm tall would be about 79,000 μm^3 which correlates well to the value calculated from the bearing area curves.

Based on this, the project team believes it has a valid approach for optically measuring the volume of material removed due to wear.

Long-Term Wear Testing

As discussed earlier, the coated piston and ring underperformed in regards to fiction benefit or robustness or both. In addition, per the discussion above, a third oil has been

substituted for underperforming components. This limits the possibilities of hardware combinations to the base piston-on-liner or base ring-on-liner with one of three oils.

This fortuitous setback actually may prove beneficial because it may resolve one of the difficulties associated with measuring material wear rates. Specifically, one difficulty that arises when measuring wear is that a tribofilm can cover the fine honing marks of a surface leading to net material gain instead of material loss. In other words, the tribofilm can mask the true material wear because it is possible that wear that can occur at a location but the tribofilm that forms offsets this wear. If this tribofilm cannot be removed, then measurements of wear may not account for the true wear rate of the material; they may either under account for the wear or actually show a net material gain.

It is well known that fully formulated oils create tribofilms that are difficult to remove, whereas the tribofilm formed from simpler formulations can be removed using ethylenediaminetetraacetic acid (EDTA) and observations of the surface underneath the tribofilm can be easily made.

It is for this reason, the project team decided that the long-term wear test will be conducted using the specially blended oil (PAO/ZDDP/MoDTC) that was formulated to achieve an ultra-low boundary friction value (oil C discussed above) and the base ring-on-liner hardware set. This combination provides the best hardware match (i.e., a hard ring on a relatively soft liner) and an oil whose tribofilm can be easily removed. The project team believes this to be the best combination to facilitate the wear measurement and to ensure an accurate reporting of material loss, material gain, and net volume. If a fully formulated oil was to be used, only net volume could be reported.

The specimens (8mm in width) were tested with the oil at a temperature of 160°C and under a 500N load to simulate engine conditions. The sample was reciprocated at 3Hz over a 20 mm stroke for varying amounts of time. The oil used was a mixture of PAO4 with 1% ZDDP and 1% MoDTC.

A Shimadzu LC-20AD pump was used to control oil flow during testing. To ensure sufficient initial lubrication, samples were given a 5-minute waiting period where no reciprocation occurred and no load was applied. The flow rate was 10µL/min for these 5 minutes, resulting in an initial 50µL of oil deposited. During actual testing, the flow rate was reduced to 0.5µL/min for the full duration of the test.

Liner segments were examined under a Bruker white-light interferometer (WLI) to obtain profilometry data. Several sites were selected for analysis using the WLI with the criterion that each site must have features that are easily recognizable so they can be located again after testing. See Figure 23.

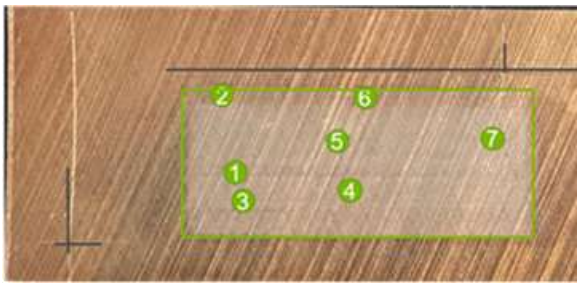

Figure 23 Locations of sites measured for long-term wear test.

The wear volume at each site was calculated after a total of 27 hours of testing had elapsed using the bearing area curve (BAC) method described in previous progress reports. The calculated wear volumes are summarized in Table 7.

Table 7 Summary of change in volume organized by rough location.

Change in 27 hour curve (μm³)			
location	left	center	right
upper	-402396	-57801	
middle	-724987	-361226	-168951
lower	-776935	-709544	

To compute the wear coefficient, K, the wear volume was averaged over the seven measurement sites to obtain an average wear volume of 457,406 μm^3. Dividing by the normal load and stroke yields a wear coefficient of 45.7 μm^3/N-m.

This value could be used in subsequent simulations in PISDYN or RINGPAK for estimating wear rates.

Reciprocating tribometer tests with the ZYNP components

Liners and rings were received by ZYNP to be tribologically evaluated. There were three variants:

- Original/Normal honing
- Z-fine - honing
- Z-fine – honing coated with C2D DLC

These were tested under a wide range of conditions using Infineum's 5W20 High FM formulation. Measurements were not performed with the high viscosity oil 10W40 oil. The friction coefficient was evaluated and the results are summarized in Table 8 for all conditions. This data will be correlated with the full-scale measurements performance by EMA and described under subtask 1.1.4.

Table 8 Summary of friction coefficient for 3 variants provided by ZYNP.

Temperature (°C)	70		100		130	
Load (N)	50	250	50	250	50	250
Original	0.10	0.10	0.11	0.11	0.12	0.11
Z-fine	0.10	0.10	0.10	0.10	0.12	0.11
C2D	0.11 No SS	0.12 No SS	0.12 No SS	0.12 No SS	0.11 No SS	0.12 No SS

The friction data was plotted as a function of time for 1-hr long tests at 70 °C, 100 °C and 130 °C, as well as 50 N and 250 N for the 5W20 High FM oil. The friction traces are shown in Figure 24.

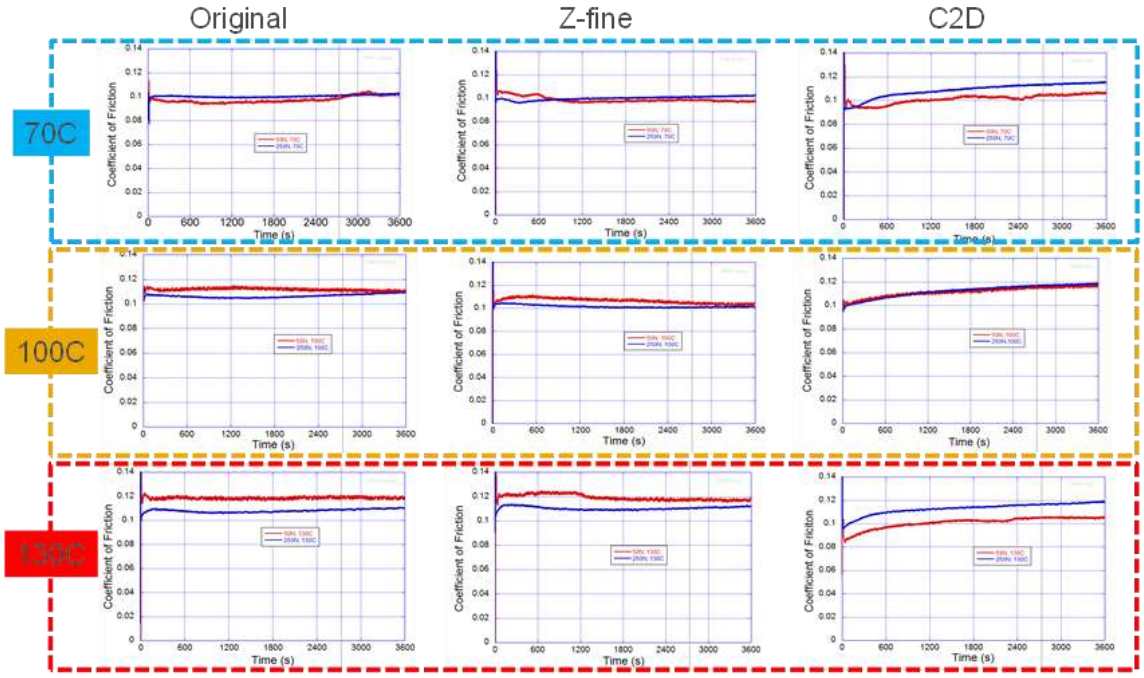

Figure 24 Friction traces over a range of conditions for the 3 variants provided by ZYNP.

Examining the results of Figure 24, it can be seen that temperature has a noticeable effect. More specifically, as temperature increases, so does the friction coefficient. That is the cases for all 3 variants. On the other hand, the load has a less pronounced effect on friction coefficient, especially at 70 °C and 100 °C. Furthermore, there is no significant difference between the baseline/original honed surface and the fine-honed surface for all data points in the matrix. However, differences between baseline and Z-fine-honed surfaces will be prominent in the mixed and hydrodynamic regimes. This can be demonstrated by maintaining a high viscosity, high speed, and low load using a benchtop tribometer. Using a 15W40 at room temperature (to maintain a high viscosity), friction waveforms were acquired at 120 rpm and 50 N. These have been plotted in Figure 25.

The graph shows that the Z-fine honing enables faster transition from boundary to mixed or hydrodynamic.

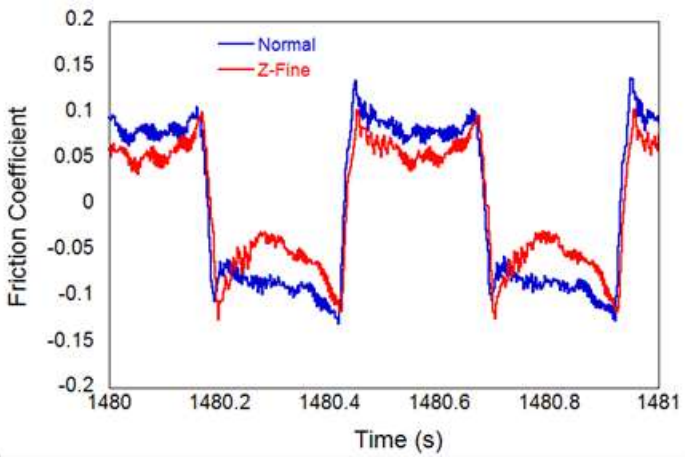

Figure 25 Friction waveforms for 2 variants.

Furthermore, it can be seen that the friction coefficient value of the C2D coating never reached a steady-state. The inertness of the surface coating may not allow for tribochemical film formation (on the liner) which might limit wear performance. This is evident in Figure 26. However, it is interesting to note that the coating survived against delamination in contrast to the first application on the Isuzu liner.

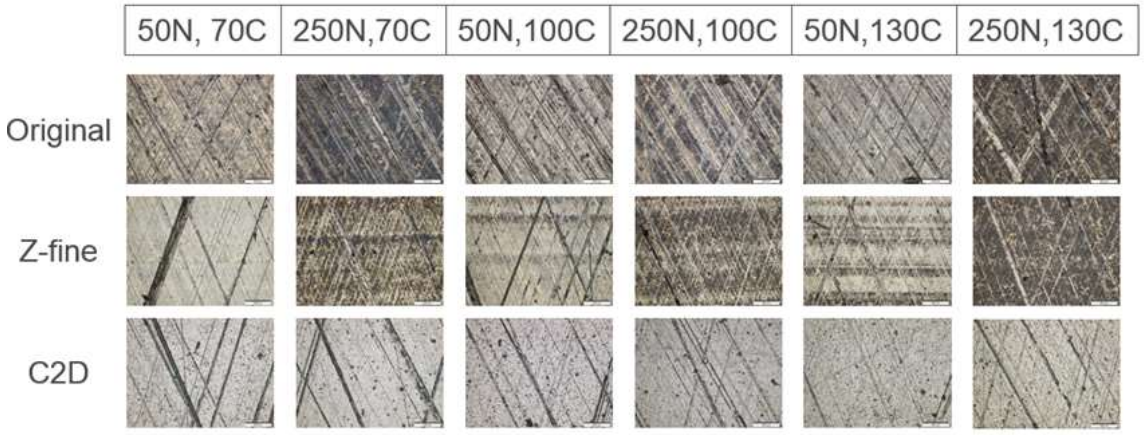

Figure 26 Optical micrographs of all liners post-test.

Additional examination of the rings revealed that the rings look intact after testing against the original liner. However, in the case when the ring was rubbed against the C2D DLC coated liner, features along the sliding direction were evident indicating that the coating might have an abrasive nature, though, quantification is very difficult and observation now can only be qualitative in nature. See Figure 27.

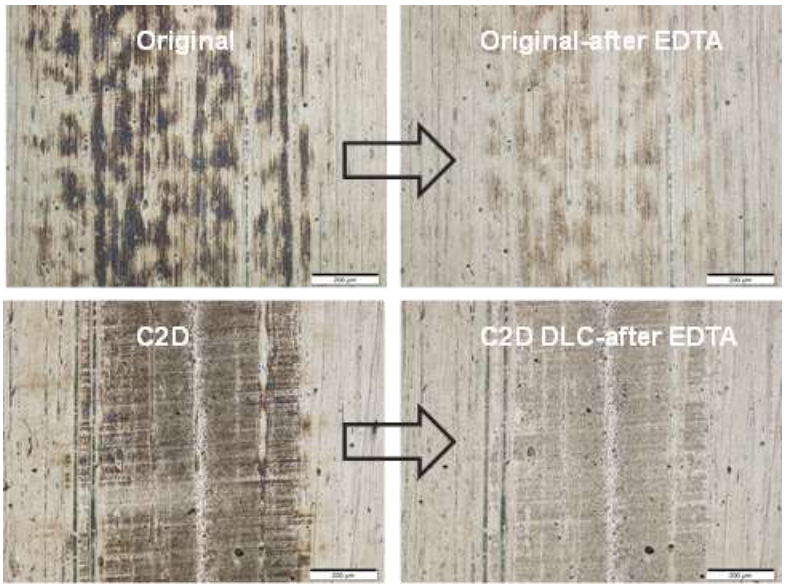

Figure 27 Ring examination post-test and after application of EDTA on the same location for the Original (uncoated) liner and the C2D coated liner.

4.4 Subtask 1.1.4 – Full-Scale Component Testing at EMA

4.4.1 Task Details

This task entails friction testing of Isuzu and ZYNP components using full-scale components not test coupons like the lab-scale testing at ANL. The data will be compared to friction coefficients obtained at ANL to understand any limitations or differences due to measurement method.

4.4.2 Task Summary

Full scale testing of the baseline Isuzu ring, cylinder bore and piston skirt has been completed but with minor exceptions which will be described shortly. The ring-on-liner data for the baseline Isuzu components is summarized in Figure 28 as function of Stribeck #. Please note the Stribeck # has been multiplied by 10^8 for convenience in plotting. The data was obtained for the two oils of interest (the high viscosity 15W40 and the low viscosity 5W20 with friction modifier (FM), at two loads (15 and 100 N) and three speeds (100, 500 and 600 rpm).

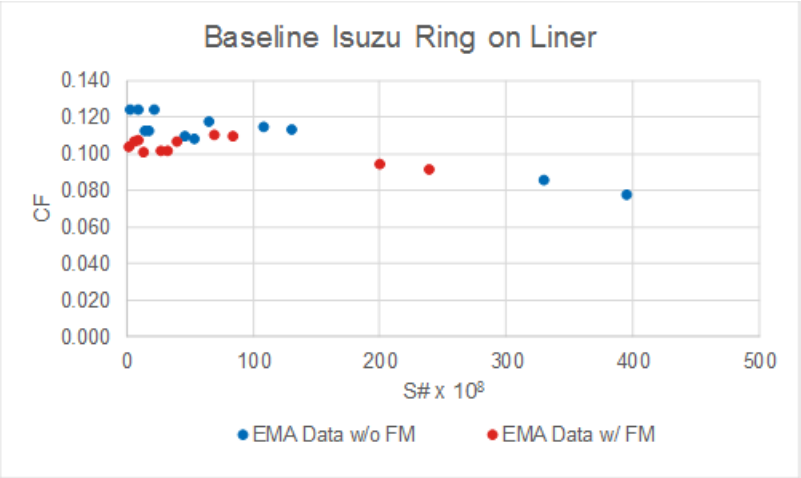

Figure 28 Summary of EMA measured friction coefficient for Isuzu baseline ring on liner.

By design, EMA's data covers a larger range of Stribeck # which should include both boundary and mixed friction regimes. As Stribeck # increases a reduction of the coefficient of friction (CF) is seen indicating that the friction regime has moved into the mixed regime.

Table 9 Comparison of EMA to ANL ring-on-liner measurements.

	EMA	ANL	% Diff
15W40	0.12	0.13	8%
5W20	0.11	0.1	9%

Conversely, ANL's data covers a much smaller range of Stribeck # to mainly capture the boundary friction regime. Extrapolating CF to a Stribeck # of zero by using only the EMA and ANL data at Stribeck # x $10^8 \leq 20$ shows that EMA's measurements are within about 10% of Argonne's (see Table 9 above).

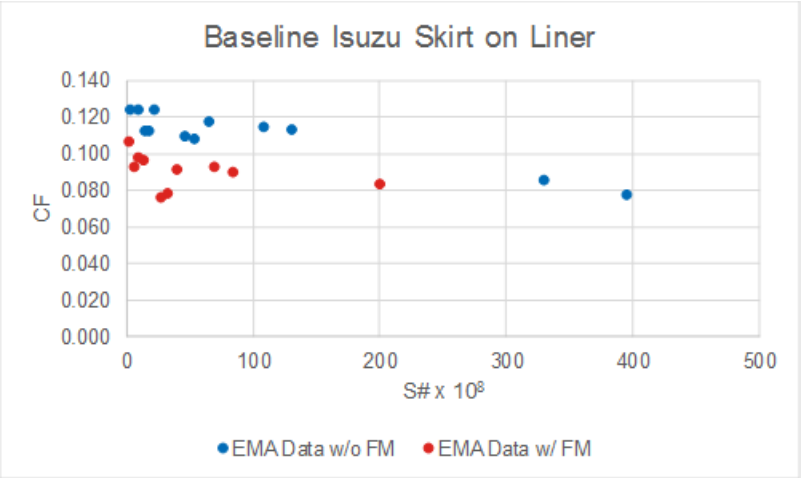

Figure 29 Summary of EMA measured friction coefficient for Isuzu baseline piston skirt on liner.

Figure 29 summarizes EMA full scale data from their skirt-on-liner tests plotted against Stribeck #. Behavior similar to the ring-on-liner tests is observed. Making a similar comparison to Argonne's measurements by extrapolating CF to a Stribeck # of zero by using only the EMA and ANL data at Stribeck # x $10^8 \leq 20$ yields the following:

Table 10 Comparison of EMA to ANL skirt-on-liner measurements.

	EMA	ANL	% Diff
15W40	0.12	0.17	42%
5W20	0.1	0.09	10%

Table 10 indicates close agreement between EMA's measurement and ANL's for the low viscosity oil with FM. However, for the high viscosity oil there is a large discrepancy. This can be attributed to the transitory behavior of the coefficient of friction observed by ANL and reported in the Q1 BY2 report. The figure illustrating can be seen in Figure 11. The duration of EMA's tests are **1200** minutes from the end of which they report steady state values. This implies that they are reporting the value of CF from a different part of the curve than does ANL. In other words, steady state is defined differently by EMA and ANL.

Please note the ANL doesn't see as much variation in the coefficient of friction for the skirt-on-liner tests when using the low viscosity oil. Steady state is reached within the first 15 minutes of testing. This explains why EMA's value correlates better to the ANL measurement for the low viscosity oil than it does for the high viscosity oil.

EMA redid the tests with the high viscosity oil (100 rpm, 130 °C and 100 N load) and recorded data after one and two hours of testing. EMA's re-test results are summarized in the following table along with a comparison against ANL's measurements:

Table 11 Summary of EMA's Re-Test of the Skirt-on-Liner Test Using ANL's Definition of Steady-State

	EMA @ 1200 minutes	EMA @ 180 minutes	ANL @ 180 minutes
15W40	0.12	0.14	0.17

From Table 11 it can be seen that correlation is improved but is still not as good as expected. EMA is probably seeing a similar transient behavior in the boundary friction coefficient as ANL had but not to the same extent.

A similar comparison of the coefficient of friction of the ZYNP components measured by ANL and EMA is shown in Table 12. Comparisons are only available for the low viscosity oil with friction modifier as ANL did not measure the coefficient of friction for the ZYNP components with the high viscosity oil.

Table 12 Comparison between ANL and EMA Boundary Friction Coefficient Measurements of ZYNP Components using 5W20 Oil w/ FM.

	Nominal Honing	Z-fine Honing	DLC
ANL	0.11	0.11	0.12
EMA	0.11	0.10	0.11

From Table 12 and from the previous comparisons between ANL's and EMA's measurements of the base Isuzu components, it can be easily seen that a good correlation has been established between ANL's and EMA's measurement methodologies. Only the skirt-on-liner measurements of the baseline Isuzu components with the high viscosity oil showed any kind of discrepancy. At this time, those skirt-on-liner measurements are considered to have a high uncertainty level. CAE simulations will have to explore the sensitivity of predictions to variations in the skirt-on-liner boundary friction coefficient.

4.5 Subtask 1.1.5 – Develop Lab-Scale Data Correlation

4.5.1 Task Details

Data regression and other modeling techniques will be used to develop improved friction (asperity) and wear correlations as a function of fundamental parameters such as the Stribeck coefficient, surface properties and oil viscosity, etc.

4.5.2 Task Summary

This task was not completed.

4.6 Subtask 1.1.6 – Development and Validation of RINGPAK Modelling Best Practice of a Lab Scale Test

4.6.1 Task Details

The purpose of this task is to develop a RINGPAK simulation best practice capable of achieving a high degree of correlation between simulation predictions and lab-scale measurements. The appropriate inputs, model parameters, assumptions, physics, boundary conditions, solver settings, etc. will be defined so that a high-fidelity simulation is achieved.

4.6.2 Task Summary

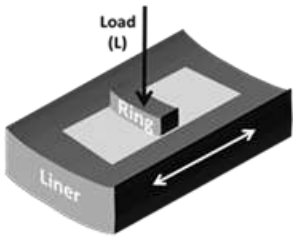

Figure 30 Illustration of the AART benchtop rig.

The configuration of the AART benchtop test is illustrated in Figure 30. It consists of segments of the top compression ring (from the Isuzu engine) that is "rubbed" back and forth against a segment of the cylinder bore. Tests have been performed at a range of loads (50, 250, and 500 N), at different temperatures (70, 100, and 130 °C, and a few at nominal room temperature), and at speeds ranging from 1 Hz up to 5 Hz (20 mm stroke).

One series in particular (test # 150707) consisted of:

- A 1 hour run @ 250 N, 100 °C, 2 Hz, 15W/40 NO FM oil to break-in the surface and establish a tribofilm on the surface (test # 150707a).
- An 8-10 minute run at nominal room temperature at different loads (25, 50, 100, 250 N) at speeds ranging from 10 rpm to 300 rpm (test # 150707b).
- A second (repeat) 8-10 minute run at nominal room temperature at different loads (25, 50, 100, 250 N) at speeds ranging from 10 rpm to 300 rpm (test # 150707c).

The runs at 100 °C exhibited nearly ‘square-wave’ behavior indicating that at 100 °C, the friction is predominantly boundary friction – little or no mixed or hydrodynamic friction (see Figure 31).

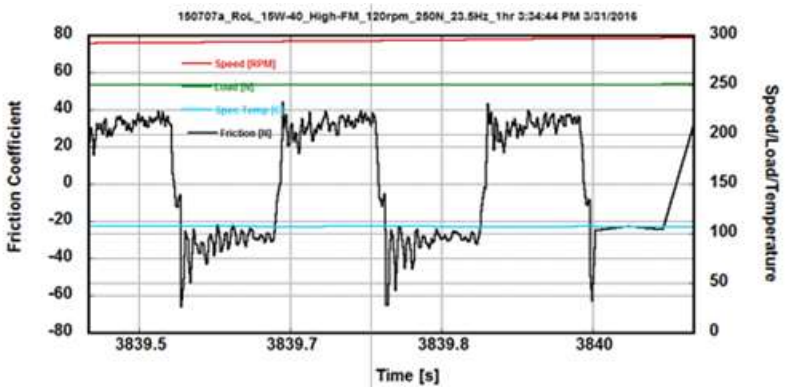

Figure 31 Friction as a function of time for a segment of time during test # 150707a (100 °C).

At room temperature however, the friction trace was 'scalloped' (see Figure 32), indicating that friction was a mixture of boundary and mixed – boundary friction at the end/reversal points where the speeds were low, and mixed at the mid-stroke where the speed and viscosity were such that partial film formation was occurring.

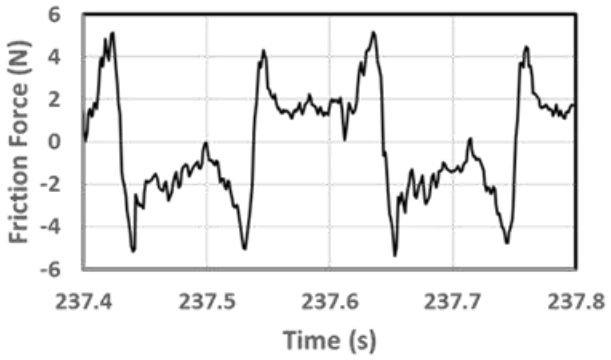

Figure 32 Friction as a function of time during a nominal room temperature run at 5 Hz (test # 150707c).

A model of the AART benchtop configuration was created in subtask 1.1.1. The model configuration is shown in Figure 33 – it consists of a piston inside of a cylinder bore with a single piston ring. The AART RINGPAK model uses an exceptionally long connecting rod (10 m) coupled with a short crank offset to simulate the short stroke of the ARRT rig. The normal force between the ring and the cylinder bore is mimicked by controlling the ring tension.

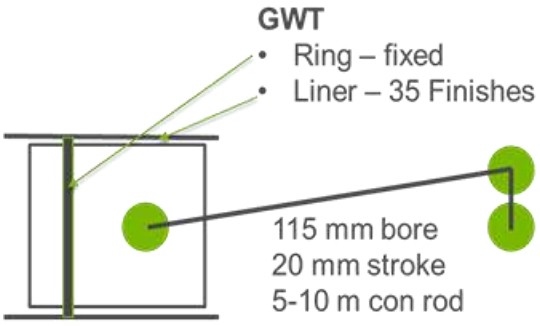

Figure 33 RINGPAK model setup to replicate AART benchtop tests.

A number of AART RINGPAK simulation runs were performed to understand the sensitivity of the friction behavior of the configuration shown in Figure 33 to various variables.

The variables that were considered in the simulation study included the following:

- Temperature: 20, 25, 30, 35, 40, 70 and 100 °C; the runs at 25, 30, and 35 °C were included to mimic the effect of friction heating at a nominal room temperature run.
- Oil: currently set at 15W/40 oil.
- Speed: 150 and 300 rpm (2.5 and 5 Hz).
- Load (F_d): 300, 600, 900, 1200, and 1500 N (2.5 to 12 N/mm).
- Inlet oil film thickness (partial film lubrication): 0.2, 1, 5, 10, and 20 µm.
- Material Dependent Parameters:
    - Asperity friction coefficient: 0.1, 0.13, and 0.15.
    - Surface finish/texture: 35 surface finishes (GWT parameters).
    - Honing parameters – honing angle.

After considerable analysis, a set of parameters were established that when used with the AART RINGPAK model would accurately predict the friction forces and traces. The data in Figure 34 shows a comparison of the experimental friction coefficient with the predicted friction trace assuming the following conditions: 40 °C oil film temperature, 0.1 asperity friction, GWT parameters consistent with an as-received liner (as estimated from MATUTIL), inlet oil film thickness of 10 µm.

Conclusions drawn from the model-experiment simulation study indicate:

- The results are sensitive to the inlet oil film thickness, especially for values below 1 µm. Values below 1 µm result in significant asperity friction and are unrealistic to the flooded condition used in the experiment. This is what caused the square

wave prediction shown in Figure 4. Above 1 µm, the results are not sensitive to this parameter.

- Ring tension has a significant effect and caution must be taken to use the correct value. Initial analysis assumed the 50 N load was distributed over a contact length of 10 mm. In reality, the contact width is dependent on a number of factors including load and radius of curvatures of the ring and bore. More detailed analysis suggests that a contact width of 6-8 mm corresponding to a unit loading of 7 N/mm (900 N F_d) is more appropriate.
- Temperature plays an important role. In particular, the role of frictional heating and surface heating needs to be considered. While friction power at the interface may be low (less than 1 watt), a simple estimate using simple conductive heat flow (-kAdT/dx = q) suggests an oil film temperature of 40 °C is reasonable even though the inlet oil temperature is at nominal conditions.
- The surface finish plays a significant role in the simulation. The agreement with the experiment in Figure 34 was achieved using GWT parameters (as derived with the MATUTIL package) for an as-received/unworn surface. When GWT parameters for the worn surface were used, the friction trace was dominated by hydrodynamic lubrication – the asperity-to-asperity friction was significantly reduced.

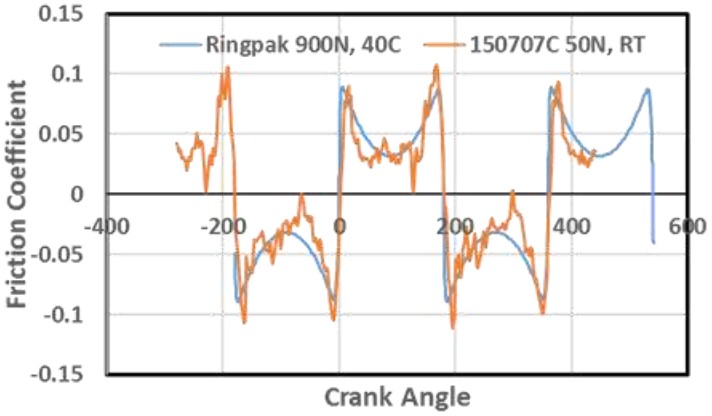

Figure 34 AART RINGPAK predicted and measured friction behaviour for 150707C.

At this point, this task has been completed, an AART RINGPAK model has been developed and validated by comparing predicted frictional behavior with observed experimental results.

4.7 Subtask 2.1.1 & 2.1.2 – Low and High Speed Motored Engine Friction Measurements

4.7.1 Task Details

This task entails obtaining the friction power from a motored engine setup without the head or other accessory components which can contribute to parasitic losses. This has the benefit of isolating only the power cylinder contribution to friction power. A full range

of speeds will be covered during this testing from engine speeds below idle to achieve Stribeck numbers comparable to the lab-scale tests all the way up to engine rated speed.

4.7.2 Task Summary

To isolate the contribution of the power cylinder components to engine friction, the friction power will be measured under motored conditions for different engine configurations (i.e., builds). The process is illustrated in Figure 35 which indicates the purpose of each build.

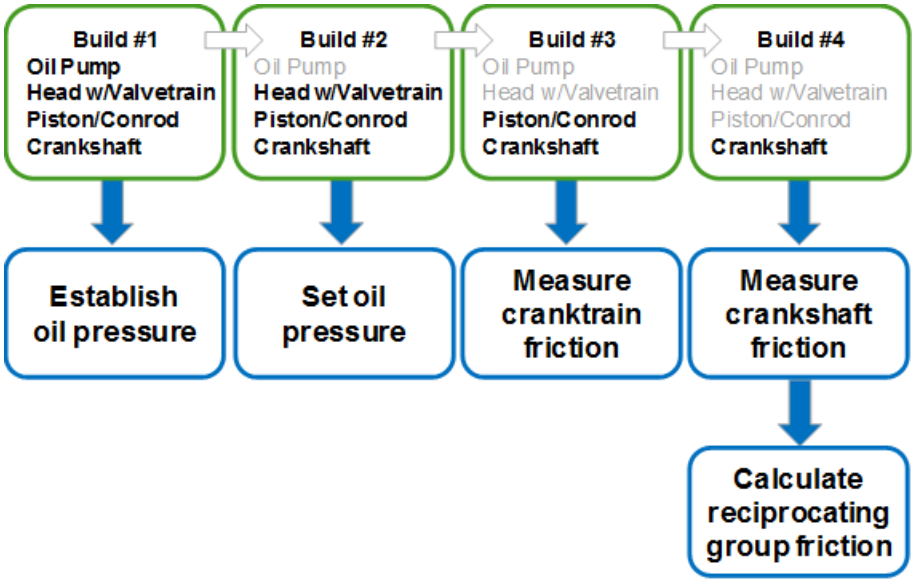

Figure 35 Build and test process for isolating friction contributions of power cylinder components.

For each subsequent build, more components are removed from the engine until only the crankshaft remains. And, at each build, the engine will be motored and the friction power measured. The engine will be motored at three temperatures for the three oils considered in this project over the speed range of the engine including some very low speeds to better match the Stribeck numbers of the lab-scale bench at ANL. The table below summarizes the current test plan which will be repeated for each oil considered:

Table 13 Test condition summary for the low and high speed motored friction tests.

Represented Condition	Nominal Temperature		Operating Speeds for Test	Conditions
	Coolant* (°C)	Oil* (°C)		
Standard Day Start Up	25	25	450, 750, 1000, 1250, 1500, 1750, 2000, 2250, 2500	Hold each speed for 30s while recording torque
Intermediate Condition during Warmup	50	50	450, 750, 1000, 1250, 1500, 1750, 2000, 2250, 2500	Hold each speed for 30s while recording torque
Baseline, Normal Running	110	110	450, 750, 1000, 1250, 1500, 1750, 2000, 2250, 2500	Hold each speed for 30s while recording torque

The expected outcome of these tests is the friction power of the power cylinder components (i.e., the difference in friction power between builds 3 and 4) as a function of engine speed, oil type, and temperature.

Build 4 removes the friction contribution of the rings and skirt but to capture the friction contribution of the crankshaft correctly, the crank still needs to be loaded with the equivalent inertia load of the rotating/reciprocating components. To accomplish this special Bob weights have been designed and fabricated with the equivalent rotating/reciprocating mass. Figure 36 shows a picture of the Bob weight.

Figure 36 Bob weight to simulate the missing rotating/reciprocating mass.

An external cooling cart is needed to continue to flow oil and coolant throughout the engine when the oil and water pump are removed at Build 2. Note that the on-engine oil cooler will be bypassed during testing. The cooling cart contains its own pumps to push oil and coolant through engine and has its own heat exchangers to control the fluid temps. An illustration of the setup is shown in Figure 37.

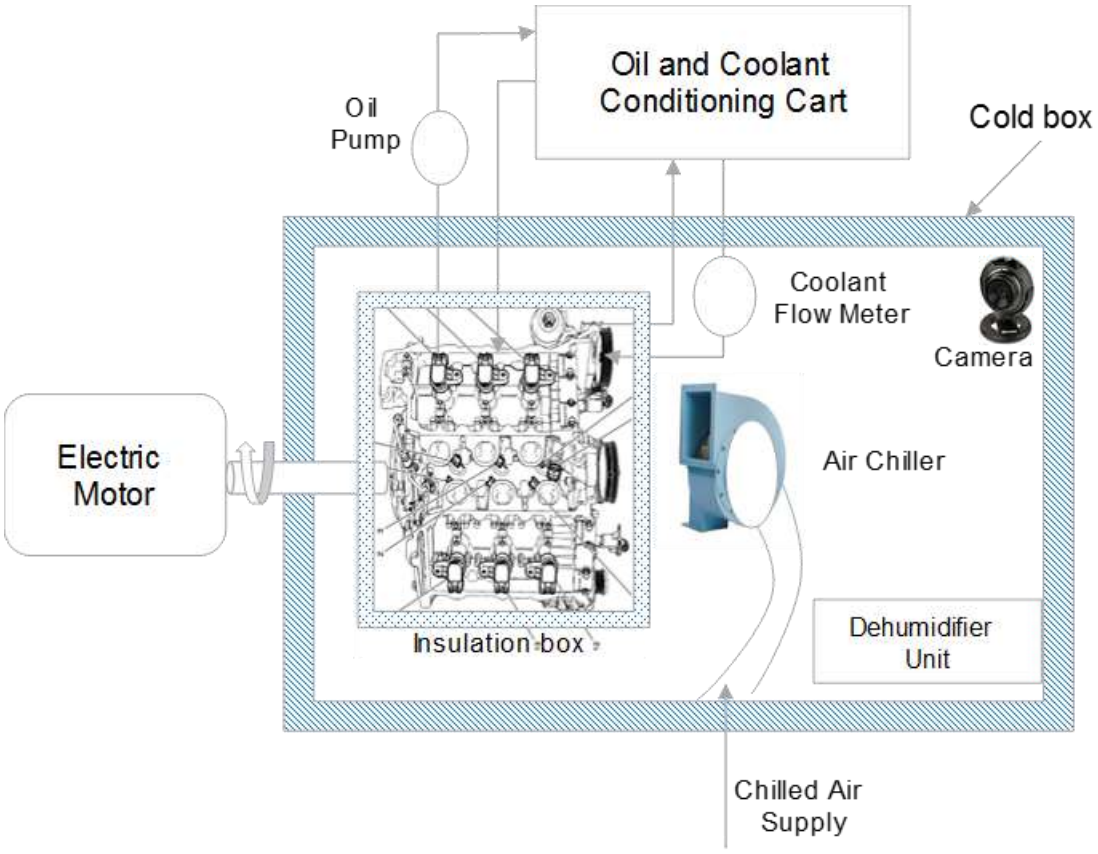

Figure 37 Illustration of the engine and cooling cart setup in the test cell.

Figure 38 shows the engine installed in the test cell and connected to the external cooling cart used for maintaining engine oil and coolant temperatures at the desired levels per Table 13.

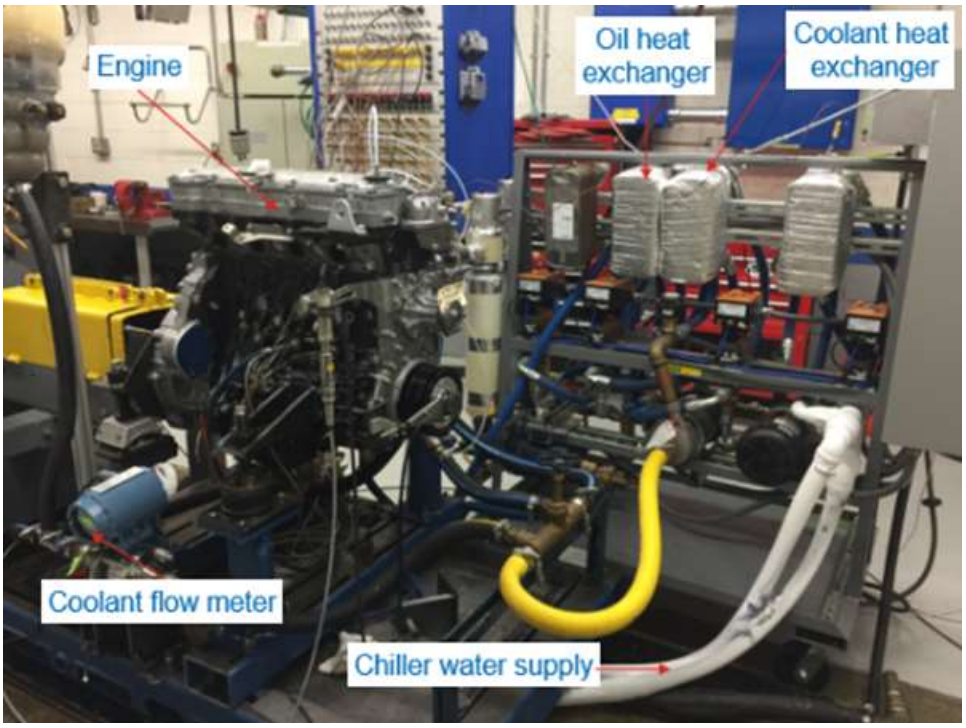

Figure 38 Picture of Isuzu engine in dyno cell with external cooling cart.

The low and high speed motored friction measurements have not without complications or compromises.

Ricardo's cooling cart struggled to achieve the targeted fluid temperatures for an engine of this size. Despite several attempts to improve the cooling capacity of the cooling cart, Ricardo was not able to consistently achieve temperatures below 25 °C. As a consequence, the 5 °C temperature condition was then dropped in favor of using of a more stable condition: 50 °C.

In addition, dyno vibration issues resulted in Ricardo limiting the low speed motored friction measurements to 450 rpm. Recall that the idle speed of the engine is 750 rpm and the target for the low speed measurements was 300 rpm based on the results of subtask 1.1.2.

As a result, the test matrix was modified again to maximize the amount of data that could be obtained within the given timing and budget constraints. Recall that three oils are considered for the testing which are summarized (again) in Table 14.

Table 14 Summary of oils tested.

Oil	Designation	COF
A	15W40 No FM	0.13
B	5W20 High FM	0.10
C	ZDDP1 + Moly Trimer	0.06

These oils were tested under the conditions shown in Table 13 according to the process shown in Figure 35.

For the nominal temperatures targeted in the motored friction tests, the temperature control was very good. This is illustrated in Figure 39 below for the Build 4 Oil C configuration. The accuracy of the temperature measurement system used ranged from +/- 0.2 °C at 25 °C +/- 0.4 °C at 110 °C.

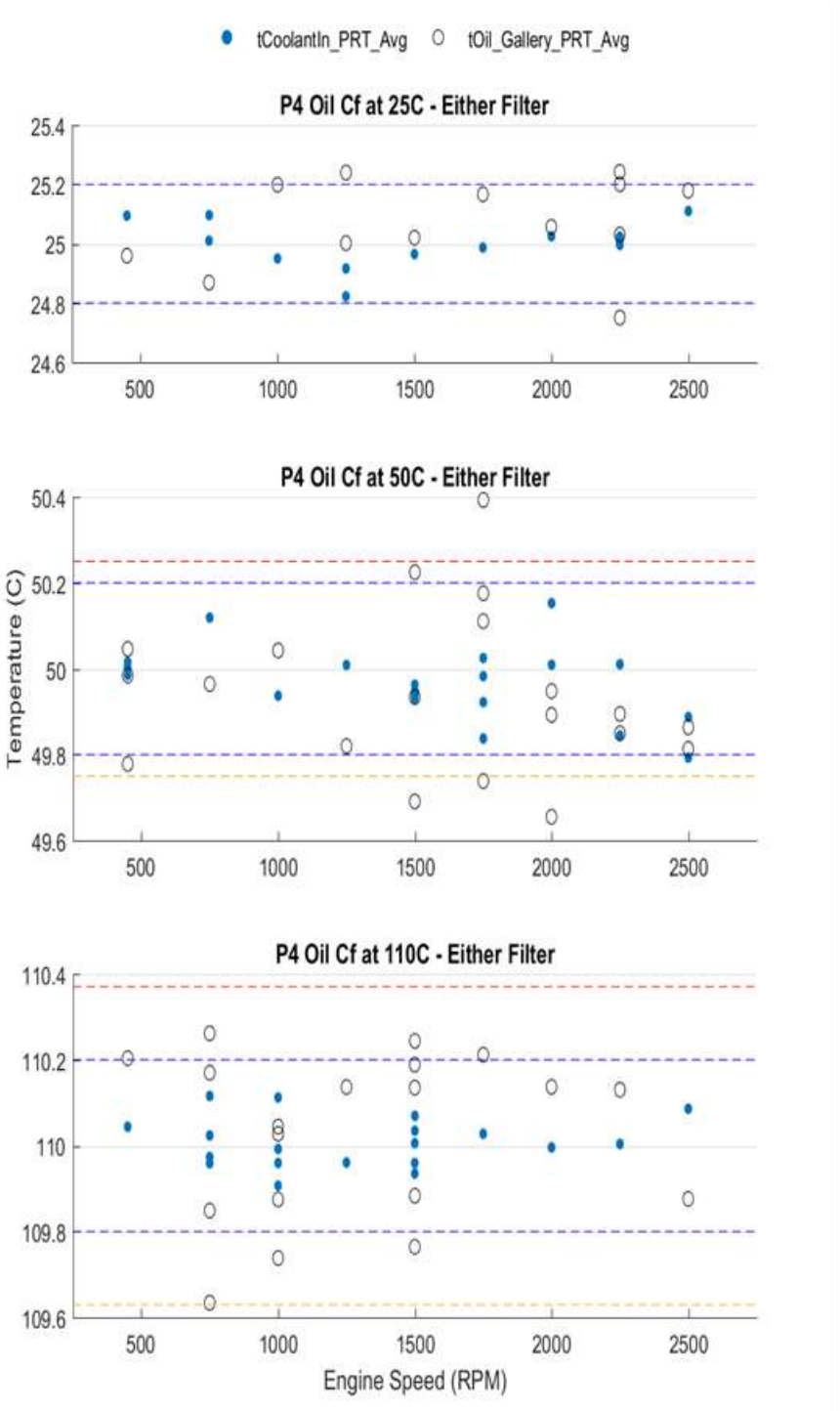

Figure 39 Temperature control capability.

A preliminary review at the raw data from the motored friction tests is shown in Figure 40. From the figure, it can be seen that the motored friction data tracks well with build,

temperature and oil: Build 1 being the full engine is expected to have the highest friction torque while Build 4, having only the crankshaft, is expected to have the lowest friction torque; higher temperatures are expected to thin the oil leading to lower friction torque; finally, at a given temperature Oil A > Oil B > Oil C in regard to viscosity.

Also, from the chart, it can be seen that there is significant difference in friction torque between builds which will improve the accuracy of the method used to calculate the friction torque associated with each component group. However, Build 4 exhibits negative friction torque which indicates a possible error in the “zero” of the torque meter. In addition, the accuracy of the torque meter is +/- 0.5 N-m and could impact the quality of data for Build 4 due to the small values of friction torque measured.

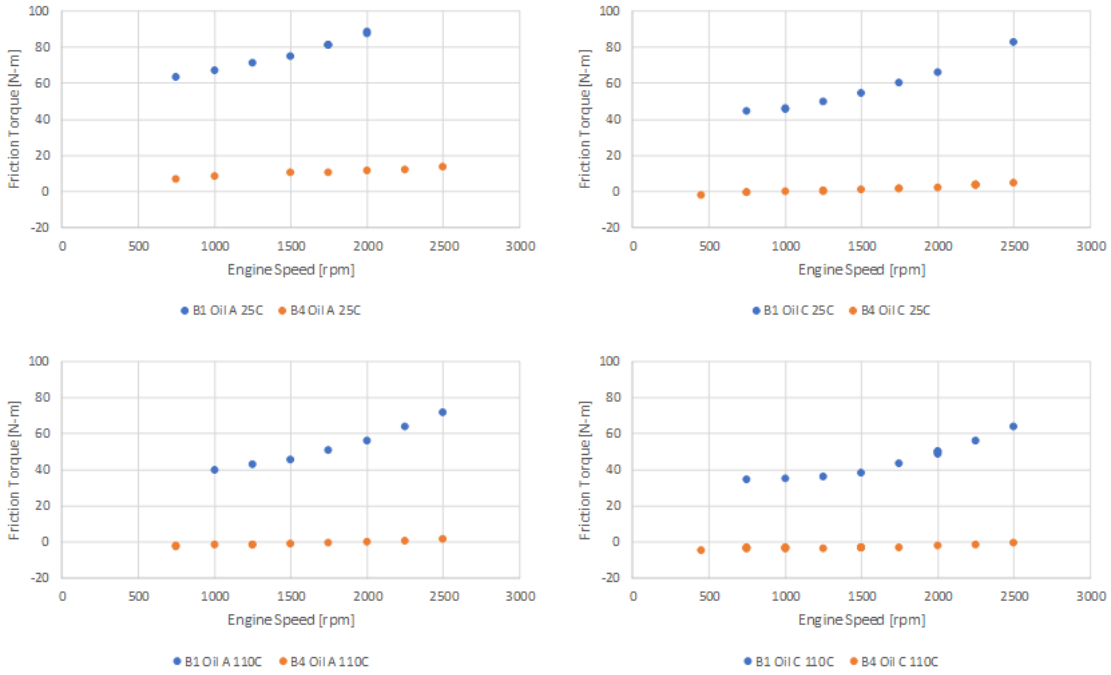

Figure 40 High speed motored friction tests for Build 1 and 4 for oils A and C at 25 °C and 100 °C.

The difference in friction torque between Build 3 and Build 4 is directly proportional to the friction of the power cylinder components (i.e., rings and piston skirt). Figure 41 shows comparison of Build 3 and Build 4 friction torque and indicates that there is a large enough change to calculate a meaningful difference.

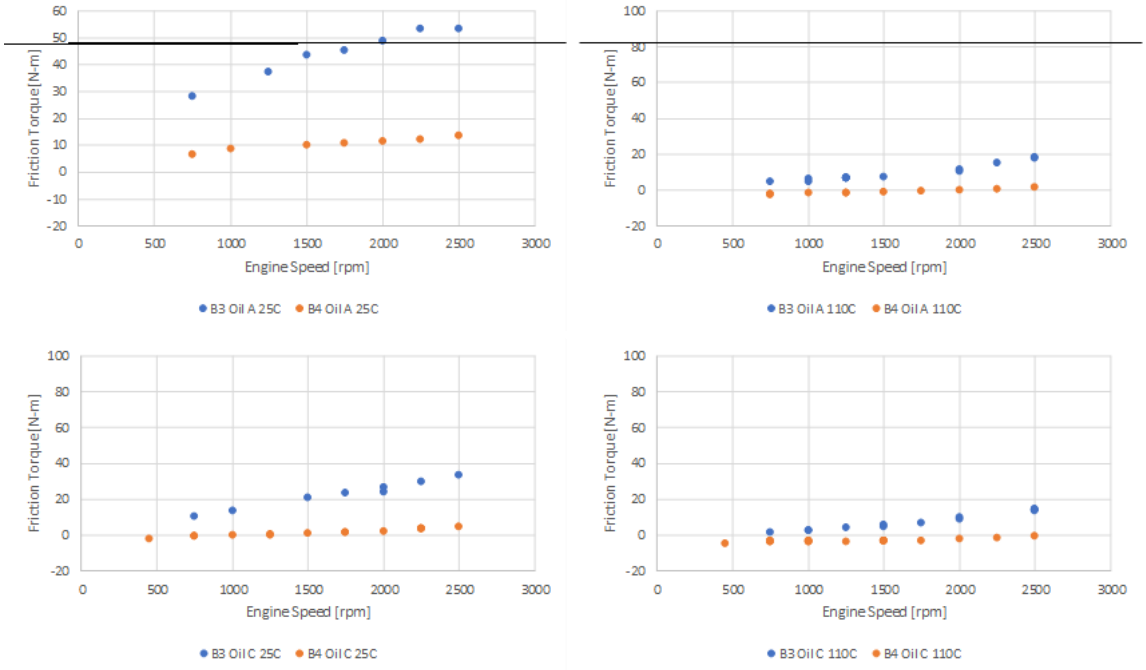

Figure 41 Friction torque comparison between Build 3 and Build 4 for oils A and C at 25 °C and 100 °C.

Finally, the friction torque quantified as friction mean effective pressure for the power cylinder components is shown in Figure 42. From the figure clear trends with speed, temperature and oil type can be observed.

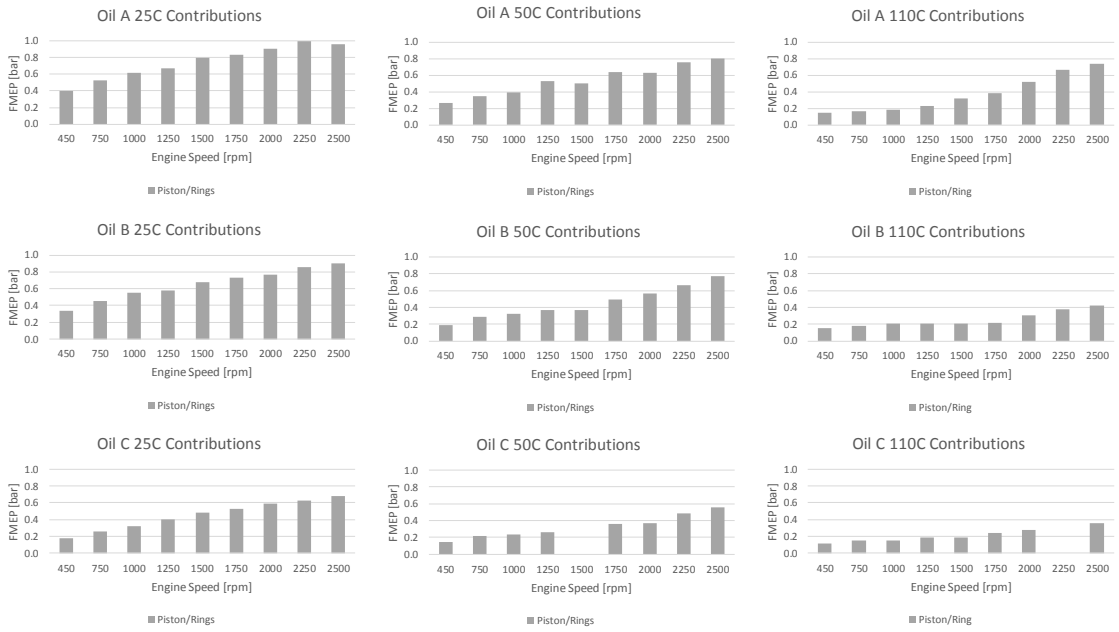

Figure 42 FMEP contribution by piston and rings for oils A, B and C at various temperatures.

4.8 Subtask 2.1.3 – Motored Engine RINGPAK and PISDYN Modelling

4.8.1 Task Details

This task entails the creation of detailed 3D RINGPAK and PISDYN models of the motored engine setup as well as correlation to motored engine tests. The task may also include modifying the simulation best practice in order to improve model accuracy.

4.8.2 Task Summary

A baseline RINGPAK and PISDYN model of the ISUZU 4H engine has been created based on the information available from Isuzu: general engine data such as bore and stroke, dimensional input data for piston, liner, connecting rod, and rings, mechanical and thermal properties for piston, liner, and rings, and surface properties for piston groove, liner, and rings provided by ANL.

Unfortunately, all of the necessary information to complete the simulation setup was not provided by Isuzu. Therefore, this task remains unfinished.

However, to test the model setup, assumptions were made for the fired engine configuration. The results from this test run are shown below in Figure 43 and are an illustration of typical results that could be obtained from RINGPAK. The top graph shows a breakdown of frictional losses by mechanism. The bottom graph shows a break of losses by individual rings. The figure also indicates that the model is working properly.

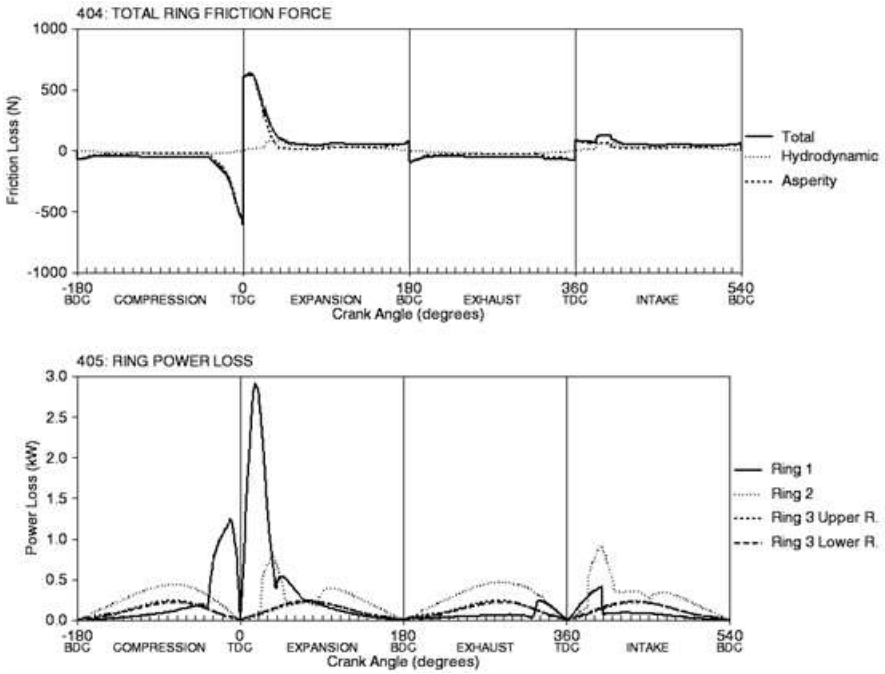

Figure 43 Illustration of full engine RINGPAK model results under fired conditions: 2500 rpm and 141 bar cylinder pressure.

Creation of the PISDYN model of the Isuzu 4H hasn't completed due to lack of information as well.

However, to test the model's functionality, assumptions were made for the clearance and component masses and the model was simulated using the same boundary conditions assumed for the RINGPAK model. The results from this test run are shown below in Figure 44 and are an illustration of typical results that will be obtained from the PISDYN. The top picture shows a spatial distribution of contact loads indicating where on the skirt where is significant friction losses (and consequently significant wear). The bottom graph is a chart of friction power loss through the skirt as a function of crank angle. The figure also indicates that the model is working properly.

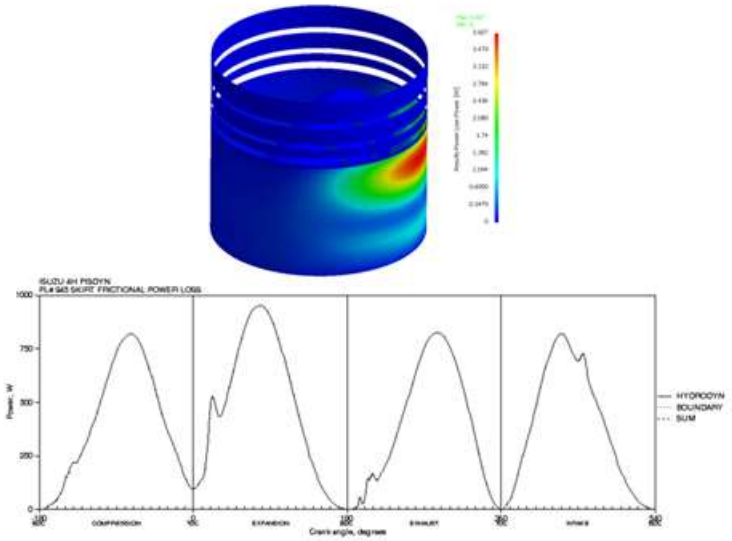

Figure 44 Illustration of full engine PISDYN model results under fired conditions: 2500 rpm and 141 bar cylinder pressure.

4.9 Subtask 3.1.1 – Thermal Survey of Fired Engine

4.9.1 Task Details

This task will provide direct measurements at various locations to map out of the engine bore and piston temperature profile which will be used for the subsequent calibration and validation of thermal simulation (subtask 3.1.3).

4.9.2 Task Summary

The engine block and piston have been machined and thermocouples (TCs) and templugs have been installed. Figure 45 shows how the engine block has been instrumented with TCs and how the piston has been instrumented with templugs.

Figure 45 Instrumented block with thermocouples (top) and piston with templugs (bottom).

The engine has been rebuilt and block temperature measurements have been made at various engine speed and load conditions.

Cylinder block temperatures were recorded along the full load curve of the engine, at engine idle, and at the peak torque and full load speed for various fueling conditions. Measurements at these operating points were repeated for different coolant temperatures: 75, 85 and 95 °C. A sample of the measurements made in the interbore region between cylinders 1 and 2 at the full load engine speed and various coolant temperatures and fueling conditions is shown for illustration purposes in Figure 46.

This data will be used to develop empirical correlations which will be used to estimate block temperatures at conditions not actually measured during the thermal survey testing. This data, whether measured or interpolated, will be used to adjust FEA boundary conditions in order to achieve a high-fidelity prediction of bore temperature and distortion.

Piston templug measurements have also been completed.

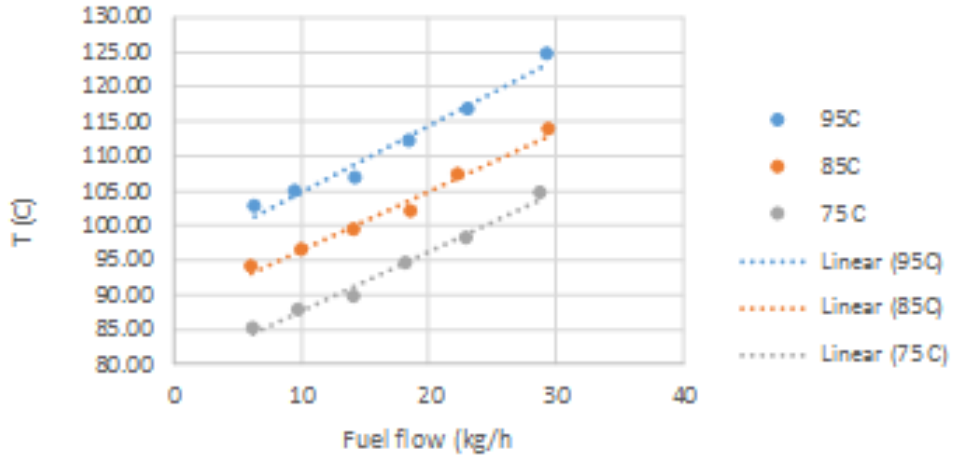

Figure 46 Block interbore temperatures at the full load speed at various fuelling and coolant temperature conditions.

Templugs were sent to Testing Engineers and Consultants, Inc. (TEC) for analysis. Specifically, TEC converted the change in templug hardness to temperature. This initial analysis has been completed and the results have been provided to Ricardo.

For reference purposes, Figure 47 shows the location of the templugs and the numbering convention used to identify individual templugs.

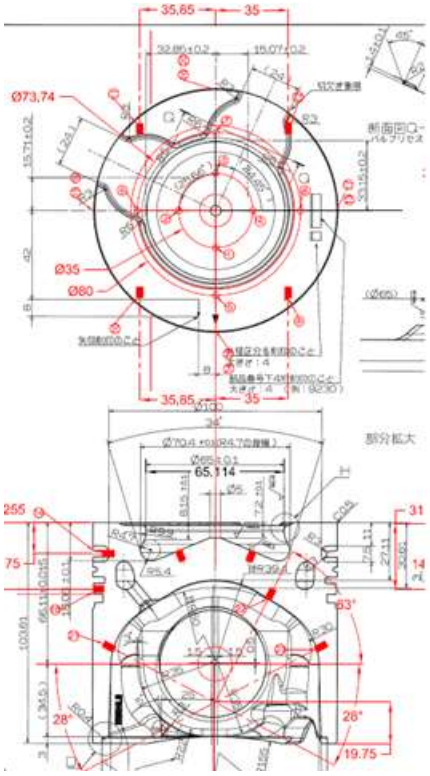

Figure 47 Templug Numbering Convention.

Figure 48 summarizes the templug temperatures and indicates the piston temperature is sensitive to engine fuelling but not sensitive to engine speed. The former trend is obvious but the latter trend was not expected since the piston cooling jet (PCJ) flow should change with engine speed and therefore so should the piston temperatures. However, a more thorough review the engine data indicated that the lube system was regulating the gallery pressure which renders the PCJ flow independent of the engine speed. It appears that gallery pressure regulation was overlooked when deciding on the test conditions for the templug measurements.

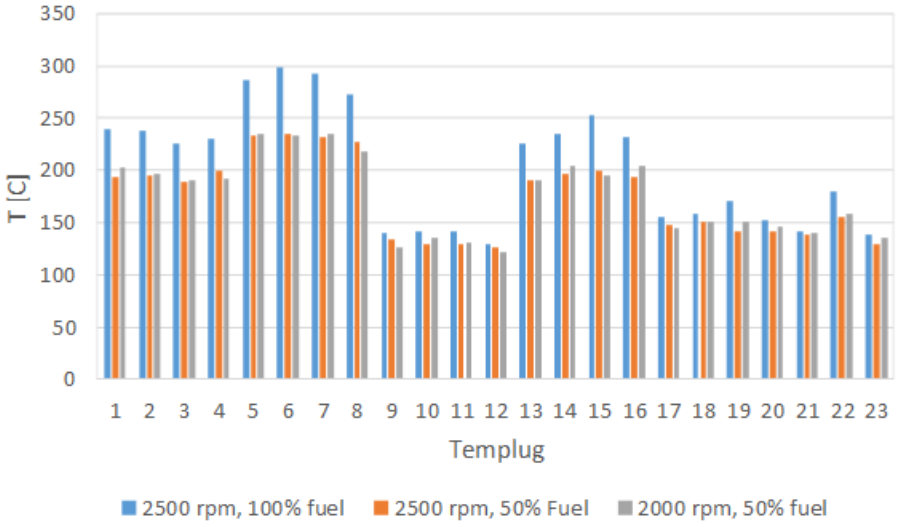

Figure 48 Piston Temperature Summary.

Despite the setback, this task is now considered complete.

4.10 Subtask 3.1.2 – Fired Engine Friction Tests

4.10.1 Task Details

Friction power will be obtained from fired engine tests performed on Ricardo's engine dynamometer. Fired engine friction measurements will be made at the same speed/load conditions as the thermal survey. Friction power will be obtained from precise measurements of cylinder pressure and brake power. Fuel economy effects will be obtained from BSFC measurements.

4.10.2 Task Summary

This task was not completed.

4.11 Subtask 3.1.3 – Fired Engine RINGPAK and PISDYN Modelling

4.11.1 Task Details

This task entails the creation of detailed 3D RINGPAK and PISDYN models of the fired engine setup as well as correlation to fired engine tests. The task may also include modifying the simulation best practice in order to improve model accuracy.

4.11.2 Task Summary

The 3D RINGPAK and PISDYN models created in subtask 2.1.3 were to be updated to reflect the fired engine condition. However, not all of the required information was

provided by Isuzu to complete the model setup. Therefore, this task remains uncompleted.

The only activity that could be completed for this subtask was the piston thermal analysis. Figure 49 shows preliminary results from a thermal analysis using uncalibrated boundary conditions based on Ricardo's best practices. The thermal analysis was conducted at the following power condition: 2500 rpm at 194hp.

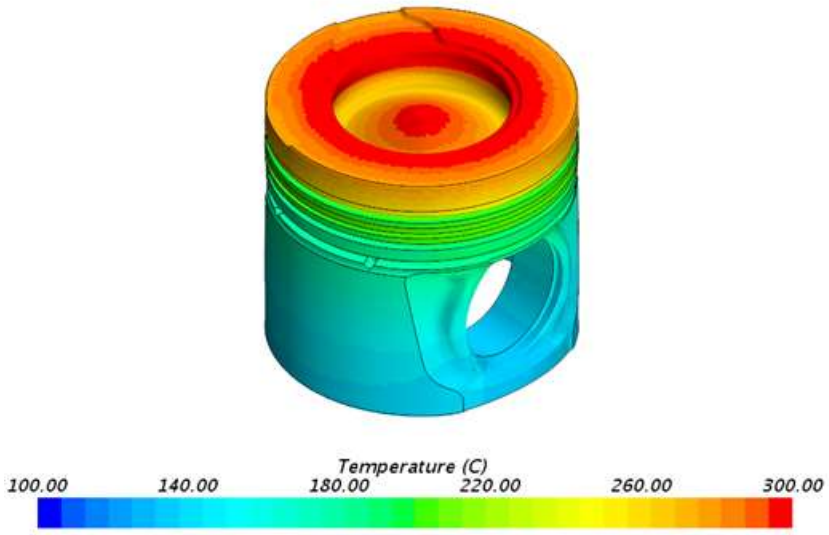

Figure 49 Preliminary Thermal Analysis of the Isuzu Piston at Rated Power Condition.

A comparison of predicted temperatures to Ricardo's recent templug measurements is shown in Figure 50. From the figure, it can be seen that temperature predictions with an uncalibrated model appear reasonable. In other words, without the templug data, one would not readily be able to detect an error in the prediction. This shows the importance of the templug measurements and model validation.

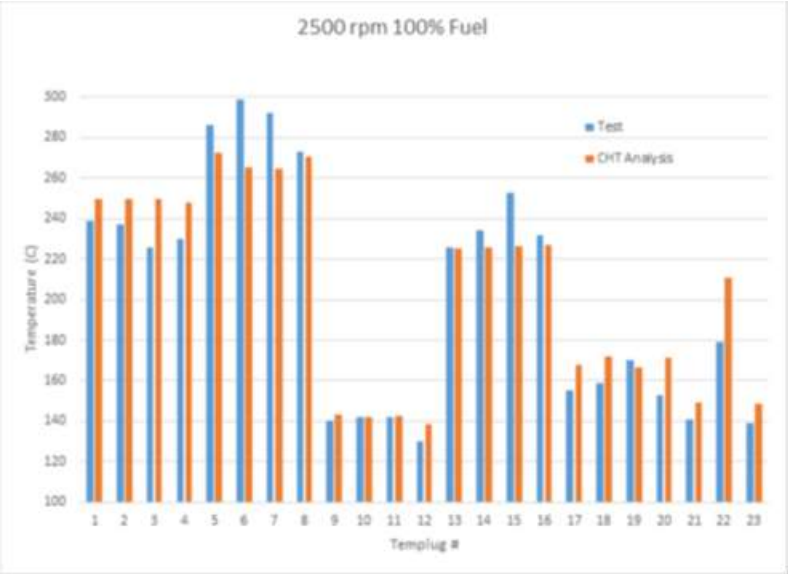

Figure 50 Comparison of templug measurements and piston thermal analysis.

Based on the available data, the oil side boundary conditions were adjusted to improve the correlation between predicted and measured piston temperatures. After the calibration, the difference between predicted and measured temperatures was less than 5%. For example, please see Figure 51 which compares the predicted and measured piston temperatures at the engine rated condition.

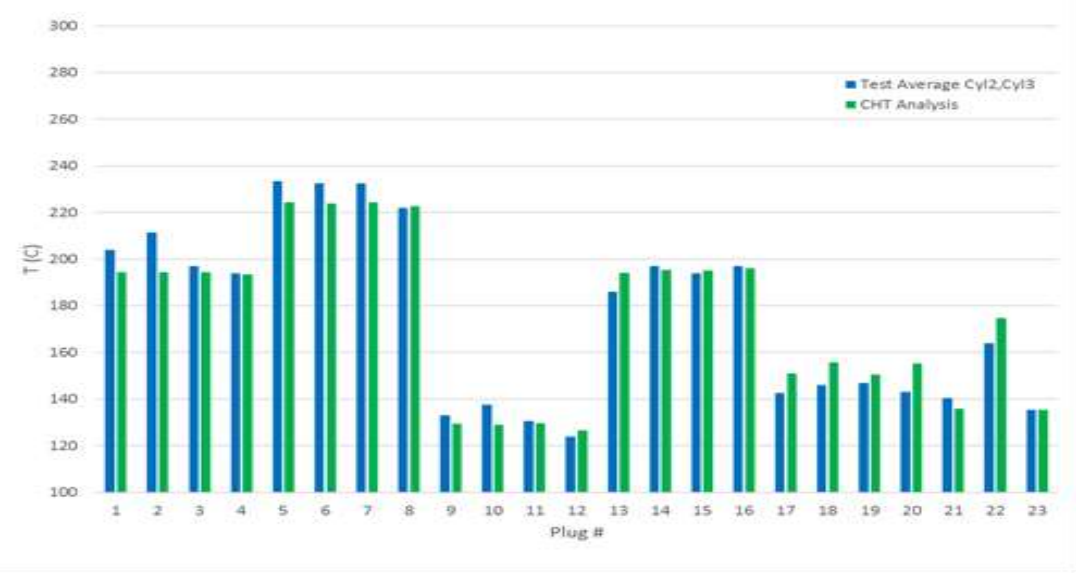

Figure 51 Comparison of the predicted and measured piston temperature at rated power condition after boundary condition tuning.

From the tuned boundary conditions, formulas were developed to allow the oil side boundary conditions to be specified at any speed or engine load. A separate formula was developed for nine critical regions of the piston: the gallery, internal skirt, external skirt, ring 1, ring 2, ring 3, top land 1, top land 2-3, and under-crown. Please note that the formulas for the combustion side boundary conditions (as a function of speed and load), i.e., at the top of the piston, were previously developed by Ricardo outside of the current project and have been used for this work.

A piston thermal prediction was made for seven key points not measured during test. Results indicated realistic trends with speed and load. See Figure 52:

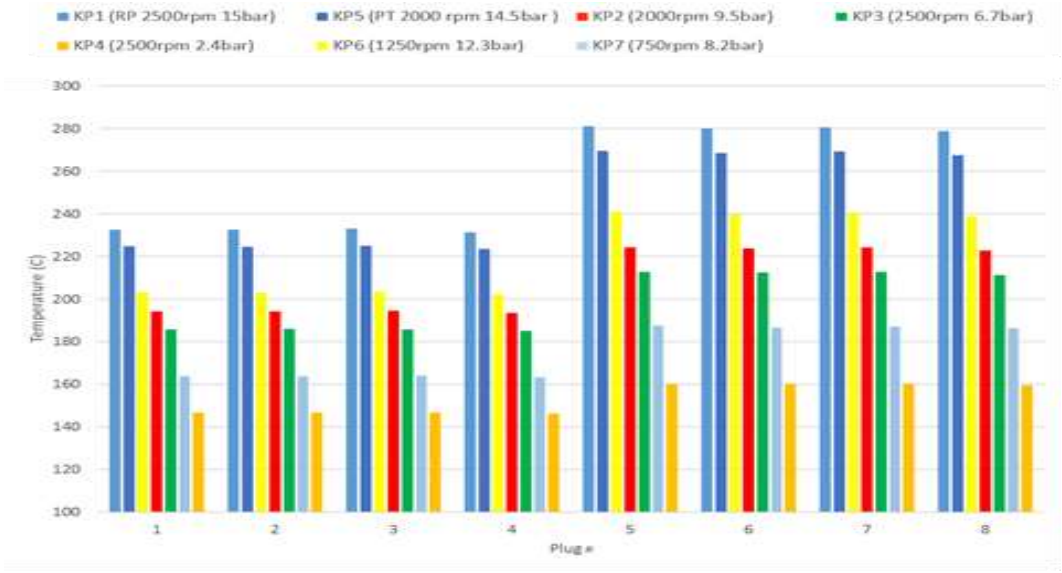

Figure 52 Piston temperature trends with speed and load predicted by analysis.

4.12 Subtask 3.1.4 – Development of Empirical Models for Prediction of Real World Fuel Economy

4.12.1 Task Details

Data regression or other modeling techniques will be used to develop a correlation between friction changes quantified by fundamental friction parameters such as Stribeck number, viscosity, surface roughness and asperity friction to changes in brake specific fuel consumption.

These models will be used to estimate the real-world fuel economy effects.

4.12.2 Task Summary

This task was not completed but Ricardo expects that the following approach could be used and would have been successfully demonstrated had the project completed as originally planned:

1. Create linear regression models of predicted FMEP from RINGPAK/PISDYN simulations (i.e., a model of a model to expand rage of applicability).

   Possible model forms used to calculate ΔFMEP:

   $FMEP_{hydro} = y_{h0} + a_h\eta$
   $FMEP_{asp} = y_{a0} + a_a e^{(-b\eta)}$
   $FMEP = FMEP_{hydro} + FMEP_{asp}$
   $(y_a, h_0, a_a, a_h) = A_0 + A_1N + A_2N^2 + A_3IMEP + A_4IMEP$
   η = viscosity
   N = Speed (rpm)
   MEP = Mean Effective Pressure (kPa); F → Friction I → Indicated

2. Validate FMEP predictions against motored engine (and fired engine) dyno testing[2].

3. Measure BSFC from fired engine dyno testing. This measurement serves as a baseline from which fuel consumption benefits would be gaged[2].

4. Through fuel consumption scaling factors (FCSF), fuel economy improvements relative to a baseline fuel economy map (step 3) from friction reduction technologies will be calculated and validated against actual fuel economy improvements from fired engine dyno tests.

   $$FCSF = (IMEP + \Delta FMEP)/IMEP$$

5. Interrogate FCSF over drive cycle to obtain real world fuel economy improvements.

5 PRODUCTS DEVELOPED

No products were developed under this agreement.

6 CONCLUSIONS

High-fidelity measurements of the coefficient of friction and the parasitic friction power of the power cylinder components have been made for the Isuzu 5.2L 4H on-highway engine.

In particular, measurements of the asperity friction coefficient were made with test coupons using Argonne National Lab's (ANL) reciprocating test rig for the ring-on-liner and skirt-on-liner component pairs. These measurements correlated well with independent measurements made by Electro-Mechanical Associates (EMA).

[2] Corrected to account for lubricant effects on non-power cylinder components contributing to FMEP or fuel consumption

In addition, surface roughness measurements of the Isuzu components were made using white light interferometer (WLI). The asperity friction and surface characterization are key inputs to advanced CAE simulation tools such as RINGPAK and PISDYN which are used to predict the friction power and wear rates of power cylinder components.

Finally, motored friction tests were successfully performed to quantify the friction mean effective pressure (FMEP) of the power cylinder components for various oils (High viscosity 15W40, low viscosity 5W20 with friction modifier (FM) and specially blended oil containing consisting of PAO/ZDDP/MoDTC) at 25, 50, and 110 °C.

One accomplishment made during this work was the development and validation of a novel technique for quantifying wear using data from WLI through the use of bearing area curves (BAC). Long term wear testing was performed for a single combination of ring, liner and a low viscosity oil to illustrate the calculation of wear rate coefficients using this technique.

Unfortunately, advanced CAE modeling using RINGPAK/PISDYN and the fired engine friction measurements could not be completed.

As a consequence, Ricardo could not develop its predictive methodology for estimating the impact of friction reduction technologies on real world fuel economy.

7 RECOMMENDATIONS

Because the project could not complete as originally planned there are no recommendations at this time.

8 REFERENCES

None.

APPENDIX 1 DESCRIPTION OF ZYNP COMPONENTS TESTED

ZYNP

ZYNP proposal for Cylinder Liner and Piston Ring technologies

Test Level	Cylinder Liner Technology	Piston Ring Technology (Cast Iron substrate material)
Reciprocating Bench Tests	Bainitic Gray Iron Slide Honing	Ceramic Chromium Coating
		PVD (CrN) Coating
	Bainitic Gray Iron Z-Fine™ Honing	Ceramic Chromium Coating
		PVD (CrN) Coating
	Bainitic Gray Iron Z-Fine™ Honing (with DLC Coating**)	Ceramic Chromium Coating
		PVD (CrN) Coating

Post Evaluations
- Friction Coefficient
- (Liner/Ring) Wear Evaluation

**DLC Coating requires project costs for third-party coating

ZYNP

Concept Description - Liners

Cylinder Liner Technology		
Bainitic Gray Iron Z-Fine™ Honing	Slide Honing – I.D. Roughness Rpk 0.3 max. Rk 0.3 – 0.8 Rvk 1.5 – 2.5	
Bainitic Gray Iron Z-Fine™ Honing	Z-Fine™ – I.D. Roughness Rpk 0.25 max. Rk 0.2 – 0.6 Rvk 1.2 – 2.8	
Bainitic Gray Iron Z-Fine™ Honing DLC Coating	Z-Fine™ plus I.D. Coating Me-DLC (a-CH) Surface hardness: 1500 HV min Thickness: 5 microns	

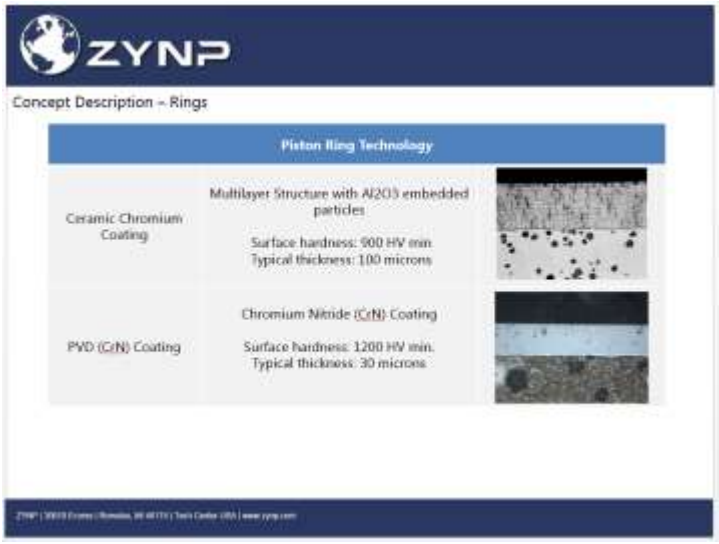

APPENDIX 2 DESCRIPTION OF EMA-LS9 RING AND CYLINDER WEAR TESTER

Specification	Value
Speed:	0 to 600 rpm (500 rpm typical)
Oiling Rate:	0.1 to 10.0 ml / hr per side (constant or ramped)
Oven Temperature:	Up to 400 Deg. C (constant or ramped)
Data Logged:	Friction vs crank angle, temperature, load, rpm, oiling rate
Stoke:	25mm typical
Sample Width:	6.35mm typical
Load Range:	20 N – 450 N (constant or ramped)

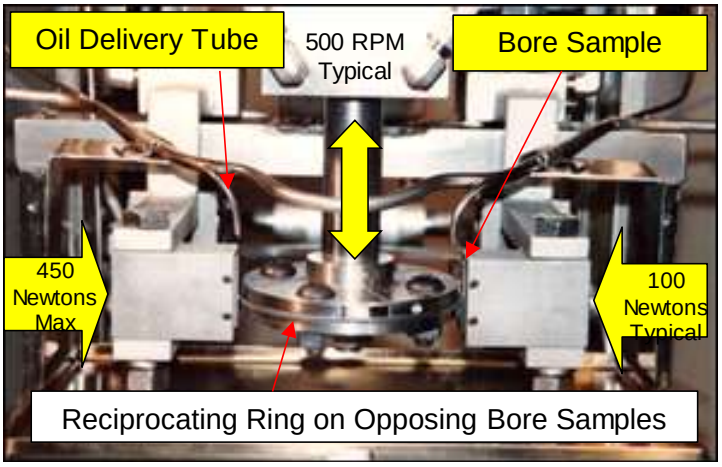

APPENDIX 3 PROJECT PARTNERS AND ROLES

RICARDO	Technical lead responsible for project management and engine dyno testing, modeling and simulation.
Argonne NATIONAL LABORATORY	Responsible for lab-scale testing, data analysis and interpretation, modeling and simulation.
ISUZU	Partner providing in-kind contributions including the engine test platform, components for lab-scale and dyno testing, and consultation
Electro-Mechanical Associates	Sub-contractor providing additional lab-scale testing
ZYNP	Partner providing in-kind contributions of components for lab-scale testing

APPENDIX 4 VISCOSITY OF OILS TESTED

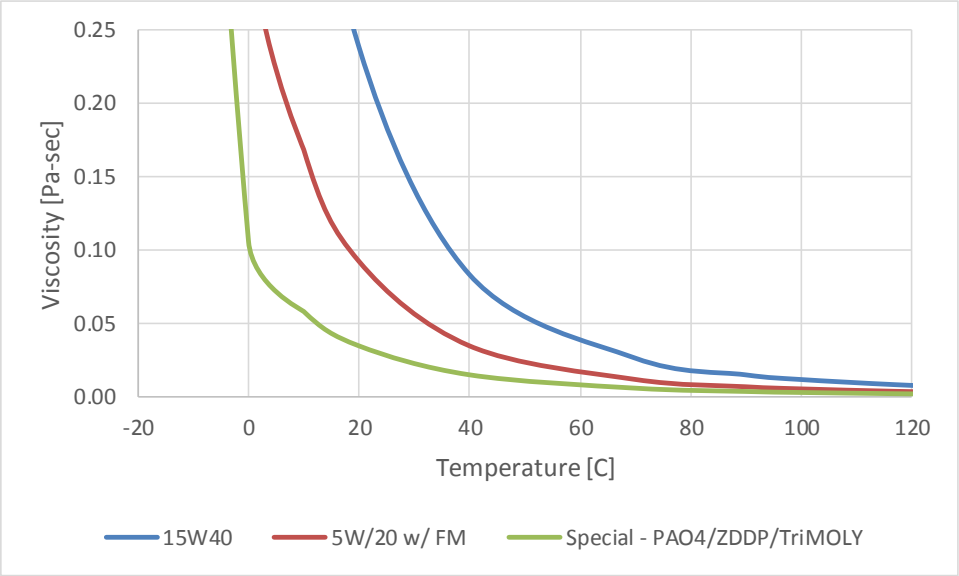

	15W40	5W20 w/ FM	Special - PAO4/ZDDP/ TriMOLY
Density	0.857 g/cc	0.849 g/cc	0.831 g/cc
40 °C Kv	98.19 cSt	42.07 cSt	18.74 cSt
100 °C Kv	13.89 cSt	7.238 cSt	4.18 cSt